HHS Public Access

Author manuscript

Adv Funct Mater. Author manuscript; available in PMC 2023 April 25.

Published in final edited form as:

Adv Funct Mater. 2022 April 25; 32(17): . doi:10.1002/adfm.202111022.

Wearable Bioelectronics for Chronic Wound Management

Canran Wang,

Ehsan Shirzaei Sani,

Wei Gao

Andrew and Peggy Cherng Department of Medical Engineering, Division of Engineering and Applied Science, California Institute of Technology, Pasadena, CA 91125, USA

Abstract

Chronic wounds are a major healthcare issue and can adversely affect the lives of millions of patients around the world. The current wound management strategies have limited clinical efficacy due to labor-intensive lab analysis requirements, need for clinicians' experiences, long-term and frequent interventions, limiting therapeutic efficiency and applicability. The growing field of flexible bioelectronics enables a great potential for personalized wound care owing to its advantages such as wearability, low-cost, and rapid and simple application. Herein, recent advances in the development of wearable bioelectronics for monitoring and management of chronic wounds are comprehensively reviewed. First, the design principles and the key features of bioelectronics that can adapt to the unique wound milieu features are introduced. Next, the current state of wound biosensors and on-demand therapeutic systems are summarized and highlighted. Furthermore, we discuss the design criteria of the integrated closed loop devices. Finally, the future perspectives and challenges in wearable bioelectronics for wound care are discussed.

Graphical Abstract

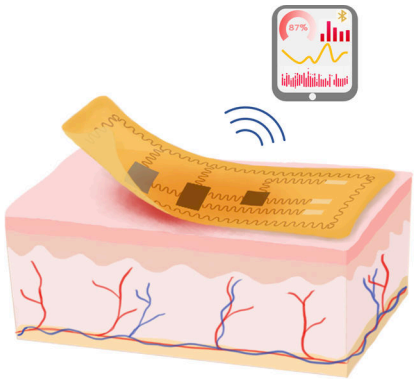

Abstract

Recent advances in wearable bioelectronics and advanced data analysis tools have created new paradigms of applications for personalized wound care. This review provides a comprehensive discussion on the advancement of device designs with a focus on wound condition monitoring,

weigao@caltech.edu .

controllable therapy, and integrated system development. We also propose the emergent opportunities and perspectives on future wearable bioelectronics for wound care.

Keywords

wearable devices; bioelectronics; biosensors; wound healing; drug delivery

1. Introduction

Chronic wounds, also known as nonhealing wounds, arise as a consequence of diabetes, decubitus, venous dysfunction, aging, and surgeries. If not appropriately managed, chronic wounds can result in infection, amputation and disabilities, and even death.[1–2] In the United States alone, over 8 million patients suffer from chronic wounds, with a financial impact of over 30 billion dollars annually.[3–4] The chronic wound conditions are highly dynamic and exhibit individual complexities impacted by various local and systemic factors. For example, diabetic ulcers stall in the inflammation phase of healing for years with the dysregulated immune system and high glucose level, increasing the susceptivity to infection. However, most commercially available wound dressings are passive and cannot provide treatments accordingly.[4] Although some dressings contain antibiotics, misapplication and long-term administration of antibiotics have led to the emergence of drug resistance in pathogenic bacteria. Platforms that can dynamically identify individual abnormities and implement controlled drug release with minimized adverse effects are required to achieve proper therapeutic efficiency of chronic wounds.

Bioelectronics can be defined as the convergence of biology systems and electronics by transducing biomedical signals into electrical signals at the tissue-electronics interface.[5–6] The first attempt to interface electronics with human tissue could trace back to 1792, when Galvani tried to apply electrical stimulation to control muscle movement.[7] Nowadays, tremendous progress has been made in the development of bioelectronics, such as biosensors, cardiac pacemakers, and neural stimulation electrodes.[8–10] One major focus of bioelectronics is wearable electronics, where the electronics could deform under small external force to maintain conformal contact with human extensive skin.[11] Recent advances in wearable bioelectronics have revolutionized personalized daily disease management beyond conventional modalities that may require long-term hospitalization or patient interventions.[12–15] Compared with the bulky nature and rigidity of traditional electronics, features such as simplified operations, flexibility, low-cost, and light weight of wearable devices can increase patient adherence which is a major challenge in clinical chronic wound care where the adherence rate is below 20%.[16–18] In particular, wearable sensors have been developed to precisely measure wound biomarkers and offer round-the-clock wound monitoring. Furthermore, recent advances in biomaterials science and digital health interventions, combined with wearable wound bioelectronics enabled local and controlled therapeutic delivery without interrupting patients' routine activities. Additionally, the large-scale manufacturing of wearable bioelectronics can facilitate patient data accumulation from multi-biomarker assessments, variable body responses, and clinical trial outcomes. Integrated with advanced data analysis tools such as artificial intelligence (AI), that

can realize an overarching goal by identifying certain recurrent patterns and potentially accelerate the decision-making process enable new modes of therapeutics in wound care.[19–20]

This review provides an overview of recent progress in wearable bioelectronics for chronic wound management (Figure 1). In particular, we first introduced the unique wound physiological features that are essential for wound-specific device configuration. Second, we summarized efforts in building wearable platforms to improve personalized wound assessment and treatments. Our focus ranged from monitoring wound biomarkers such as physical signals, biomolecules, and microorganisms in the wound extrudates, as well as on-demand delivering therapeutic strategies such as responsive drug delivery systems (DDS), controllable electrical stimulations, and thermodynamic therapies. We also presented systems-level integrated designs leveraging technologies such as wireless communication and closed-loop control algorithms for the next generation of wound therapies. Finally, we discussed challenges and perspectives on the future of applying wearable bioelectronics for chronic wound care.

2. Wound-specific design considerations

Achieving reliable functions of bioelectronics at the wound sites relies on appreciating the complexity of the wound microenvironment. The multifaceted process of wound healing involves various cells and metabolites in a distinct aqueous milieu, which may result in mechanical or electrical failure of the device. On the other hand, the tissue-electronics interactions can affect cellular behaviors such as migration, proliferation, cell-cell interactions, and immune responses, which may delay the healing process or cause tissue damage.[21] Additionally, constant and conformal contacts between bioelectronics and wounds are required for accurate sensing and optimal therapeutic outcomes.[22] This section discusses the biochemical compositions and mechanical properties that need to be considered when designing bioelectronic devices for wounds.

2.1 Chemical environment

Maintaining the performance of bioelectronics is challenging and can affect the long-term durability of the device in the humid wound microenvironment. Wound fluid is a complex solution containing different ions, metabolites, and enzymes that can vary according to wound types and healing stages. For instance, in acute wounds and the initial stages of wound healing, the environment is acidic with a pH value in the range of 4–6. In contrast, chronic wounds are basic with pH values in the range of 7–9 due to the alkaline accumulation.[2] The increase of pH creates a favorable environment for bacterial growth, which results in further pH elevation at the wound bed.[2, 23] The pH fluctuation should be considered when designing therapeutic devices for drug release. Moreover, following the tissue damage, the level of reactive oxygen species (ROS) commonly increases, which function as oxidants and degrading polymers. ROS elevation and bacterial contamination can also lead to an increased enzyme release caused by cell apoptosis and inflammation.[24] For instance, keratinocytes secret matrix metalloproteinases (MMPs) to degrade the extracellular matrix (ECM) for re-epithelization.[25] The high MMP concentration can also

lead to the degradation of collagen-/gelatin-based biomaterials. Such properties could be utilized for controlled drug release systems. In comparison, inert materials are preferred for long-term treatment since some chronic wounds remain in the inflammatory stage for a long time and create non-healing wounds.

The breathability of bioelectronics contributes to the gas exchanges between wounds and the external environment and maintains certain wound moisture, which is essential for the healing process. Poor breathability may cause exudate accumulation, increasing the susceptibility to infection.[26] In contrast, excessive evaporation elevates wound dehydration risk.[27] An optimized water vapor transmission rate can lead to the highest healing rate.[28] Therefore, controlling breathability should be considered when designing wound bioelectronics. For example, porous electrode substrates have received much attention for wound care due to their ability to adjust thermal-moisture exchanges.[29–30] Another approach to remove excessive wound fluids is to utilize directional fluid transferable materials with a self-pumping function enabling it to control the wetness.[31–32] In addition, the process of biosensing may require extraction of wound exudates into the device for sampling and analysis. It is essential to control the velocity of fluid collection to avoid wound dehydration, which will hinder the healing process by decreasing oxygen and nutrient delivery. Also, some sampling modules deploy microneedle arrays to collect fluids, which may cause further damage to the wounds and surrounding cutaneous tissues.

2.2 Immune responses

Immune cells heterogeneity and their communication with fibroblasts play a key role in the wound healing process. The prolonged inflammation process at chronic wounds can last for months, increasing the susceptibility to infection. Reducing foreign body response (FBR) at the material-tissue interface is one primary concern to maintain device performance and prevent scar formation.[33] At the beginning of FBR, acute inflammation will be induced by provisional matrix formation and protein absorption on the implanted bioelectronics surface. Innate immune cells such as phagocytes, mast cells, and neutrophils adhere to the devices, secrete cytokines (e.g., interleukin-6 (IL-6), IL-8, transforming growth factor–β1 (TGF-β1)), increase acidity, and elevate local ROS concentration, potentially causing device damages.[34] Later, the lymphocyte infiltration, foreign giant cell formation, and fibroblasts activation lead to granulation and eventually fibrous capsule development around the devices.[35–36] Additionally, poor material biocompatibility can lead to excessive inflammation. For example, oxidizing agents or photoinitiators are widely utilized to transfer materials into reactive forms or for polymerization reactions. Incomplete removal of these toxic reagents can directly cause apoptosis and tissue damages, recruiting inflammatory macrophages and increasing cytokine secretions.[37–38] Non-immunogenic biomaterials at the wound-bioelectronics interface are required to reduce protein absorption and toxic agent release.

On the other hand, proper immune responses can accelerate wound healing. For example, Griffin et al. changed the chirality of MMP-degradable peptides in the hydrogel matrix, activating adaptive immunity.[39] In a mice model, the chirality alteration MMP-peptide induced an immune response that mediated progressive tissue remodeling, hair follicle

neogenesis, and reduced fibrosis.[40] Despite the identifications of immune factors such as macrophage polarizations that control the balance between skin regenerations and fibrosis, quantitative analysis of immune biomarkers in the wound is necessary to improve wound bioelectronics designs.[41–42]

2.3 Mechanical compliance

Mechanical properties of the tissue in wounds change in different healing stages. For example, an elevation of stiffness can be observed during the remodeling stage due to the enhanced collagen expression. Despite the dynamic changes in stiffness during wound healing, wound tissues are generally soft, with elastic moduli of 10–100 kPa.[43–44] It is essential to design wound bioelectronics with appropriate stiffness and stretchability. Extracellular mechanics can influence cell behaviors such as proliferation, migration, and differentiation.[45–46] For instance, soft materials could increase ROS-mediated cellular signaling pathways in mesenchymal stromal cells and accelerate the healing process.[47] Comparatively, the rigidity of many current electronics, such as silicon with E >100 GPa, can cause mechanical stress, tissue damage, excessive inflammation, and scar formation.[21, 48] Additionally, skin – particularly at joints and wrists – can experience up to 30% mechanical deformations during routine activities. Thus, a similar elasticity as local native skin is required for applied bioelectronics to avoid mechanical or electrical failures and generate highly reliable signals.[49] Recent advances in materials chemistry (e.g., conducting polymers,[50] and liquid metals[51]) and microfabrication techniques (e.g. meandering architectures,[52] and metallic bucking[53]) can benefit wound bioelectronics designs to achieve desired mechanical properties.

2.4 Adhesion

Tissue adhesives can be used to apply bioelectronics to the wound in a stable and conformable manner. However, the wound fluid serves as a physical and chemical interfacial barrier, that hinders the development of robust interfacial adhesions.[54] Covalent and noncovalent bonds between devices and underlying tissues are established to overcome these challenges.[55–56]

Figure 2A demonstrates a tissue adhesive strategy based on hydrogen bonds. Hydrogen bonds are comparatively weaker than chemical interactions.[57] To achieve better adhesions, Chen et al. adopted the *N*-[tris(hydroxymethyl)methyl]acrylamide (THMA) to increase the bonding density. As it illustrates, the hydrogen bonding clusters in a crosslinked hydrogel can dissipate energy, both on the surface and in the bulk hydrogel. The hydrogels prepared with 80% THMA displayed maximum adhesion energy of 422 J m^{-2} (Figure 2B), which is a significant improvement when compared to physical interaction-based adhesives as control (10 J m^{-2})).[58]

For covalent adhesions, carbodiimide reagents such as *N*-Hydroxysuccinimide (NHS) and 1-ethyl-3-(3-dimethylaminopropyl) carbodiimide hydrochloride (EDC) are widely used due to their spontaneous and rapid reaction with the amine and thiol groups at the tissue interface. As Figure 2C shows, an adhesive surface of wound dressing formed with chitosan as a bridging polymer and a carbodiimide reagent as a coupling agent.[59] A dissipate matrix

was formulated with poly(*N*-isopropyl acrylamide) (PNIPAM) and alginate to enhance the adhesion. Adhesion energy of 175 J m^{-2} was achieved (Figure 2D), which can be further improved to more than 1000 J m^{-2} by increasing the PNIPAM ratio.[58] Such adhesive dressings could directly accelerate the healing process via active contractions. Similarly, Shagan et al. reported a heat-triggered wound glue with NHS-modified four-armed polycaprolactone (star-PCL).[60] After being extruded from a glue gun, the gel rapidly solidified and exhibited excellent adhesive properties, which can be potentially used for bioelectronics and wound interface.

Dry e-bioadhesive interfaces offer an alternative solution to overcome the drawbacks of conventional adhesives (i.e. non-conformal contact, unstable adhesion, and scar formation). (Figure 2E).[61] The adhesion process contained two sequential steps: **i)** The carboxylic acid groups in the e-bioadhesive removed surface fluids by hydration and swelling, and formed intramolecular bonds with tissues; **ii)** NHS ester groups established covalent bonds for stable adhesion.[54] Using this technique, a rapid adhesion was achieved in 5 seconds with >270 J m^{-2} interfacial toughness for skin (Figure 2F). The adhesive layer was integrated with graphene to further enhance its conductivity, making it suitable for different bioelectronics applications.

A tremendous number of biomaterials have been developed for tissue adhesions. It is crucial to design adhesives according to the wound microenvironment. Some key design criteria for bioadhesive used in wound interface includes biocompatibility, robust and long-term adhesion in the wet environment, and compatibility with electronics functions. For instance, monomers or degradation byproducts of synthetic polymers, such as cyanoacrylates, can be toxic, hindering continuous contact with wounds.[56, 62]

2.5 Wound characteristics

The desired specifications of wound bioelectronics are also determined by wound characteristics, including location, depth and size of the wound. Physical and chemical properties of the skin (e.g., impedance, moisture, thickness, etc.) vary throughout the body. For example, the thickness of the dermis is almost 1 cm on the back, compared to less than 1 mm thickness of the eyelid dermis. Furthermore, the abundance of cutaneous blood vessels, nerves, glands as well as subcutaneous muscle and fat layer components varies from different wound locations. The wound location and depth can also influence drug penetration and required dosing amount. Thus, these characteristics are crucial for precise evaluation of wound conditions, diagnosis, and choosing treatment options. In addition, to minimize possible side effects on adjunct healthy skin, it is to tailor bioelectronics shapes and sizes in accordance with wound geometry. Recent advances in manufacturing technologies such as 3D printing and laser cutting allow precise and highly personalized wound bioelectronic designs.

3. Biomarker sensing and monitoring

Electronic biosensing and detection is one of the most developed areas in the bioelectronics field. Current biosensors are mainly developed based on the covalent modification of electrodes with responsive materials and sophisticated biological components to

enable label-free detections of physical and biochemical signals. Recent advances in biosensors enabled the detection of various physiological biomarkers at wound sites. Unlike conventional diagnosis that requires off-body sample preparation, time-consuming analysis, and largely depends on the clinicians' judgments, wearable biosensors can provide real-time wound monitoring with quantifiable outputs. Also, the direct readout from *in situ* sampling and analysis requires minimal patient intervention and largely improves patient adherence, which are essential for early detection of pathology conditions such as dehydration and infection of wounds. Furthermore, the diverse cell interactions and dynamic wound microenvironment require a comprehensive analysis of different biomarkers, which is extremely challenging via traditional approaches. Developing multiplexed biosensors can draw valuable conclusions by acquiring sufficient information with minimal sample preparation. For instance, bacterial culture, which is the current gold standard for infection diagnosis, lacks sufficient sensitivity and may present a false negative result at the early stage of infection.[63] In comparison, using wearable biosensors to assess wound biomarkers (e.g., temperature, pH, and bacterial toxins) allows a comprehensive real-time analysis. By leveraging progress in biotechnology, materials science, analytical chemistry, and engineering, biosensors can provide multiple physical, small molecular, macromolecular, and microorganism signals with high fidelity and fewer labor-intensive processes to guide clinical decisions.

3.1 Physical signal sensors

3.1.1 Temperature sensors—Temperature is considered as one of the twelve classic signs in the Clinical Signs and Symptoms Checklist (CSSC) for chronic wound assessment.[64] Human skin temperature varies between 34 and 37 °C. Generally, an increased temperature is associated with bacterial infection or excessive inflammation, while temperatures lower than 33 °C indicate a delayed healing process due to inhibited cell activities and metabolisms. Thus, dynamic and quantitative measurements of local temperature are crucial for wound management.

One feasible approach to measure wound temperature is using resistance-based temperature sensors, These sensors work by adopting thermoresistive materials such as metals (e.g., gold,[65] nickel,[66] and copper[67]) and semiconductors (e.g., graphene[68] and silicon[69]) as key elements. For example, a laser-guided graphene (LGG)-MXenes/PDMS temperature sensor was developed and displayed on human skin (Figure 3A and 3B).[70] As the temperature rises, the PDMS electrode exhibited a thermal expansion, resulting in an enhanced electron-photon scattering and increased resistance.[71] This temperature sensor showed a linear positive temperature coefficient of resistance (TCR) in a range of 25–50 °C, which made it suitable for wound temperature monitoring (Figure 3C).

As demonstrated in Figure 3D, Lou et al. engineered an integrated wireless wound monitoring system by incorporating a miniaturized band-gap temperature sensor STH21.[72] This device showed an excellent accuracy (<0.1 °C deviation) at the physiological temperature range in a pig wound model. Figure 3E shows the stable working state of the implanted device on a full-thickness wound. After inoculation, a temperature elevation

was observed at the wound site several hours earlier than body temperature, suggesting the capability of the patch in the early detection of wound infections (Figure 3F).

In clinical settings, a visual temperature sensor that enables convenient observation is desirable. However, sophisticated imaging cameras are required for precise readouts, resulting in high manufacturing costs and inconvenience for long-term wound surveillance.[76] Therefore, the visual sensors can be coupled with other approaches for visualization and precision. For instance, Najafabadi et al. developed a wound temperature sensor by combining a thermometer strip with a silver-based thermistor.[77] When the temperature exceeded 37 °C, the strip color changed for visible warning, while the thermistor displayed quantitative signals simultaneously.

Different thermosensitive materials can be used for wound temperature sensors with stable and real-time measurements. However, only a few electrochemical sensors are capable of distinguishing temperature values at the wound site from adjunct skin. Moreover, the temperature values may also vary in different areas of the wound. Customized fabrication to suit irregular wound shapes as well as temperature mapping technologies can greatly advance the future applicability of wound temperature sensors.

3.1.2 Impedance sensors—Impedance detection is a tool for determining the physiological conditions of the skin, particularly for subcutaneous tissue damage (closed wound). A pressure ulcer is a common chronic closed wound that affects millions of patients in the United States with a severe morbidity rate.[78] Unlike open wounds, the initial stage in pressure ulcers is not visible, which makes the early detection challenging. Pressure ulcers are associated with ischemia and tissue damage, resulting in an elevated conductivity due to ion-rich cytoplasm release from dead cells. Therefore, measuring skin impedance allows early detection of the underlying ulcers.

Swisher et al. developed a flexible gold electrode array for impedance mapping (Figure 3G).[73] After applying the sensor on a rat pressure-induced tissue damage model, magnitude and phase angle spectrum were measured (Figure 3H and 3I). They were also able to detect the differences in impedance between wounded and healthy tissues at a lower frequency. With a determined damage threshold value, they obtained an early damage prediction map immediately after applying the pressure. Histology results further confirmed the correlation between impedance and ulceration (Figure 3I). These findings validated the feasibility of utilizing impedance sensors for the dynamic assessment of pressure ulcer risk.

Combining surgical sutures with biosensors provide a promising approach to monitor wound conditions and promote healing simultaneously. Figure 3J and 3K exhibit a battery-free suture-based capacitive sensor to detect deep wound integrity through the frequency and power changes of received signals.[74] The efficacy of tissue integrity sensing was further evaluated on mice muscle wound with simulated gastric leakage and suture breakage (Figure 3L). There was significant change of resonate dip (Δf = 400 MHz) when applying simulated gastric leakage. A significant change in the power received (20 dB) as well as disappearance of resonant dip were observed after suture breakage. In addition, it was also verified that the

bioelectronic sutures showed equivalent healing outcomes in comparison with medical-grade surgical sutures.

Impedance values can be also used to detect the level of skin hydration,[79] cell viability,[80] and cell migration.[81] For example, Pei et al. reported a continuous wound impedance measurement on a pig wound model by integrating a wireless processing part with an impedance sensor. They observed a correlation between impedance and both the healing process and wound types.[82] Further investigations on the complex relationships between impedances and wounds may bring promising opportunities and improve patient care.

3.1.3 Pressure sensors—Pressure sensors can provide timely alerts of excessive mechanical stress applied to the tissue, which is essential for ulcer prevention. It is estimated that 19%–34% of diabetic patients develop diabetic foot ulcers (DFUs) in their life.[83] The international guidelines recommend footwear pressure sensing to prevent DFU recurrence.[84] While impedance sensing provides early warning immediately after tissue damage, pressure monitoring can notify patients to offload high pressures and prevent ulcer development.

Mechanisms for skin pressure measurement are generally based on converting pressure to electric signals, such as capacitance, piezoresistivity, and piezoelectricity. Among them, capacitive pressure sensors are more stable in response to temperature alteration.[85] Figure 3M presents a smart insole system with a 24-channel capacitive sensor array for static and dynamic plantar pressure mapping.[75] By patterning the dielectric layer film with hexagonal pores, a sensitivity of 12×10^{-3} kPa^{-1} in the range of 0–200 kPa was achieved due to appropriately increased permittivity. Intuitive heat maps were displayed for the plantar pressure under three different standing postures in Figure 3N.

Piezoresistive pressure sensors are also widely developed due to the ease of fabrication and simple operation processes. However, piezoresistive materials mostly exhibit a negative resistance variation against external forces, restricting their operating range.[86–87] To overcome this limit, Wu et al. engineered a positive piezoresistive plantar pressure sensor with laser-scribed graphene.[88] Under the applied pressure, random cracks were appeared between graphene layers, resulting in a sharp resistance increase. The positive resistance-pressure correlation property endowed the sensor with > 360,000% resistance change rate and a sensitivity of 12.3 kPa^{-1} at 200 kPa.

Notably, ulcers are progressively developed rather than caused by an instantaneously applied pressure. Abbott et al. conducted a randomized proof-of-concept clinical study to investigate the function of a plantar pressure sensor with active feedback and self-direct adjustment modules (SurroSense Rx, Orpyx Medical Technologies, Canada) in diabetic patients.[89] The sensor was designed to record the static high pressure and warn the user, rather than focusing on the highest peak plantar pressure. They reported that a less frequent ulceration rate in the intervention group when compared to the control group, suggesting direct contributions of static pressure in planar ulcer developments. Combining different types of pressure signals as well as other biomarkers is required for a more accurate and efficient ulcer management.

3.2 Small molecule sensors

3.2.1 pH sensors—The pH value is considered as a critical biomarker for wound sensing, due to its essential role in various biochemical interactions. High pH is associated with bacterial colonization, while acidity indicates a healing state with balanced protease activities, optimal fibroblast migration, and effective ECM remodeling.[90] Generally, pH-responsive polymers such as polypyrrole and polyaniline (PANi) are widely used due to their capability of reversible protonation and deprotonation as well as excellent sensitivity (> −50 mV pH^{-1}).[91–92] Figure 4A and 4B demonstrates a paper-based pH sensor with Ag/PANi-emeraldine base (EB) composites, capable of transition into emeraldine salt (ES) form with increased conductivity in response to pH drop.[93] The fabricated electrodes were integrated with a potentiostat and a commercially available bandage. In addition, the PANi impedances showed a frequency-independent behavior at 10–100kHz when the device was applied on wound extrude models (Figure 4C). A calibration curve of pH versus impedance values was obtained to quantify pH.

Apart from polymers, pH-sensitive metal oxides with rapid proton absorption capabilities such as SnO_2 and IrO_2 have shown high sensitivities as well (~ −50 mV pH^{-1}).[94] However, their high cost and poor biocompatibility may impede their broad application. Colorimetric approaches by incorporating with pH sensitive dyes (e.g., universal indicators and phenol red) have also enabled visualized pH sensing.[95–96]

3.2.2 Uric acid (UA) sensors—Wound uric acid concentration ranges from 220 to 750 μM.[98] Elevated uric acid levels (> 500 μM) indicate wound severity with excessive ROS and inflammation, while decreased uric acid suggests bacterial colonization as a result of microbial uricase expression.[98–99] Currently, uric acids can be detected via non-enzymatic and enzymatic approaches.[100] Sharp and colleagues reported an anodized carbon fiber mesh to detect urate by square wave voltammograms. In their sensor, urate concentrations correlated with the heights of peaks at +0.23V for quantifiable analysis, covering a range of 0–500 μM. However, interferences from other metabolites and the narrow detection range limit its applicability. To overcome these challenges, enzymatic sensors were developed by immobilizing electrodes with uricase. Figure 4D represented an electrode utilizing uricase to oxidizing uric acid into allantoin for electrochemical sensing.[70] A linear detection range of 50–1200 μM was observed with a sensitivity of 422.5 μA mM^{-1} cm^{-2}, satisfying the wound sensing demands (Figure 4E).

3.2.3 Oxygen pressure (pO_2) sensors—Wound oxygenation plays a vital role in determining healing outcomes. Proper reduction of oxygen activates the hypoxia inducible factor-1α (HIF-1α) signaling, which promotes angiogenesis and re-epithelization.[101] However, chronic and extreme hypoxia delays cell proliferation and increases the susceptibility to infection.[102] Generally, a pO_2 value of >40 mmHg is sufficient to support the healing process, including collagen depositions, bacterial defense, and fibroblast proliferation.[103–104] Ruthenium- and palladium-based materials are the most commonly used materials for O_2 sensing, owing to their oxygen-responsive phosphorescence features.

Figure 4F demonstrates a wound bandage coupling an oxygen sensor with an oxygen generator for therapeutic purposes.[97] To fabricate the sensors, they developed a ruthenium compound ($Ru(dpp)_3Cl_2$) based ink for inkjet printing. They reported that the fluorescence lifetime of the ink reduced from 4 to 2 μs in response to an oxygen concentration increase from 5 to 25 mg/L. The obtained oxygen concentrations were correlated with H_2O_2 perfusion-induced oxygen generation on mice wound models (Figure 4G). Moreover, the light wavelength for their phosphorescent ink excitation was in the visible range, to minimize potential tissue damage. Similarly, Marks et al. formulated a paintable pO_2 sensing bandage for postsurgical wound management.[105] The patch contained a commercial liquid bandage, palladium-porphyrin for oxygen sensing, and a fluorescein reference dye. The sensor showed a wide sensitivity range (0–160 mmHg). Furthermore, a correlation between pO_2 measured from the bandages and blood oxygen saturation was observed on patients. Such liquid bandage configurations were compatible with a variety of current commercial wound dressings, suggesting a tremendous translational potential for clinical application.

3.2.4 Glucose sensors—Diabetes mellitus delays normal wound healing through a series of the hyperglycemia-induced pathological processes, including proinflammatory state, tissue hypoxia, osmotic diuresis, impaired vascularization, and peripheral neuropathy.[106] It is recognized that wound glucose levels display a solid correlative relationship with blood glucose, which can provide crucial therapeutical guidance for clinical treatment. Human wound glucose concentration varies from 0 to 7 mM.[107] Currently, both electrometric and colorimetric approaches can be utilized for glucose sensing.

A variety of non-enzymatic glucose sensors are developed by using metals, metal oxides, and alloy-metals as sensing materials. For example, Li et al. engineered a Cu-Ag superstructure for glucose sensing based on glucose amperometric responses, yielding a sensitivity of 7745.7 μA mM^{-1} cm^{-2} and a limit of detection (LOD) of 0.08 μM.[108] However, the poor selectivity of non-enzymatic sensors dampens their performance in the wound milieu, which contains a myriad of metabolites and oxidants. Currently, glucose oxidase (Gox) has been widely used in fabricating enzymatic sensors, which oxidizes glucose into gluconolactone. For instance, Ohayon et al. presented a GOx-functionalized n-type polymer coupling the functions of glucose sensing with anodes of biofuel cells.[109] As the GOx catalyzed glucose, anodes emulated the doping voltage for glucose detection with an outstanding LOD of 50 nM. Simultaneously, the generated electrons traveled to cathodes and reduced H_2O_2. This provided a solution for autonomous sensing with month-long stability, which is a highly desirable feature for long-term wound management.

Enzymatic reactions can be also used in combination with redox-sensitive dyes for colorimetric sensing. Figure 4H demonstrated a fluorescent glucose sensor fabricated by encapsulation of GOx, horseradish peroxidase (HRP), and dichlorofluorescein (DCF) within a zwitterionic poly-carboxybetaine (PCB) hydrogel matrix.[96] The superhydrophilicity of zwitterionic materials minimized the interferences of the hydrophobic enzymes, resulting in higher stability of the encapsulated proteins.[110] The hydrogel matrix could be also modified by incorporating pH-responsive phenol red dye for pH and glucose dual sensing (Figure 4I). *In vivo* studies further confirmed the stability of the glucose sensors and the correlation between wound and blood glucose levels (Figure 4J).

Recent advances in small molecule sensing can provide crucial information to guide clinical diagnosis and therapy of wounds. However, several roadblocks are remaining for their practical implementation. Despite the excellent specificity of the enzymatic approaches, the delicate bioactivity of enzymes limits their long-term monitoring reliability. The pH of wound fluid is dynamic, which may deactivate and even denature enzymes. Therefore, it is essential to choose enzymes that can tolerate a wide pH range. Stable and biocompatible material systems are also required to avoid any interference with the enzyme function. Another challenge comes from the complicated healing process. For example, considering that inflammation and ROS levels increase are involved in acute wound healing, it is necessary to distinguish them from the normal healing process. In addition, high inter-patient and wound type-based variation of metabolites concentrations and pH value may cause complications in the result analysis. Comprehensive analysis with other biomarkers may benefit further classifications.

3.3 Macromolecule sensors

3.3.1 Protein sensors—Many proteins are secreted by cells that participate in the healing process or released after cell apoptosis, serving as significant indicators of wound conditions. Currently, immunoaffinities (e.g., aptamers and antibodies) are utilized for protein sensing.[111–114]

Recent advances in the systematic evolution of ligands by exponential enrichment (SELEX) enabled the development of aptamers for versatile recognitions of biomolecules and even microorganisms.[115–116] By modifying aptamers with redox reporters through covalent bonding, aptasensors offer an adaptable platform to a wide range of targets.[117] In the work by Gao et al. (Figure 5A), aptamer-functionalized graphene-gold electrodes were integrated into a patch with a microfluidic wound extrudate collector.[118] A panel of inflammatory mediators (tumor necrosis factor–α (TNF-α), IL-6, and IL-8) and healing status biomarker (TGF-β1) were selected for wound surveillance. After applying the sensors on patients with venous ulcers, the personalized correlation matrices of these biomarkers and wound sizes were obtained (Figure 5B). Pasche et al. demonstrated a sensor for optical detection of C-reactive protein (CRP), by coating its ligand on the electrode surface.[119] CRP concentration is another essential indicator of wound infection, and its increase is heavily correlated with bacterial colonization. The immunoaffinity between CRPs and ligands has changed the hydrogel refractive index and enabled CRP level detection.

Aptasensors can provide an approach to detect biomarkers irrespective of their chemical reactivity, but several limitations should be noted and addressed. On one hand, although aptamer binding affinity is responsive to many triggers (e.g., pH, temperature, and light), the redox-based process of electrochemical sensors is irreversible.[120] The operation time of the electrochemical sensor mainly depends on the aptamer loading capacity, resulting in long-term hypersensitivity. On the other hand, considering the environment light interferences in the optical sensors in practice, real-time calibration and readouts are required for reliable and continuous applications. In recent years, natural receptor-based sensors have been developed that may resolve these issues. For example, G protein-coupled receptor (GPCR) family can specifically detect various stimuli such as peptides, glycoproteins, fatty acids,

and nucleotides.[121–122] The activation of GPCRs results in their conformational changes and downstream hydrolysis of guanosine triphosphate (GTP), which can be transmitted into electric signals for long-term quantifiable analysis.[123] However, most natural receptors are based on integral membrane proteins, and artificial lipid membranes are generally required to maintain their stability and reusability.[124–125] Further investigations in designing binding pockets-mimicking peptides could be beneficial. Finally, significant improvement is needed to develop continuous and durable protein sensors with facile fabrications.

3.3.2 Nucleic acid sensors—Nucleic acid-based sensors are another promising approach to detect bacterial and viral species at the wound sites. Recent developments of isothermal amplification technologies such as recombinase polymerase amplification (RPA) can execute efficient nuclei acid amplification at 37–42 °C, which is in the range of body temperature.[129] Figure 5C demonstrates a bandage-like RPA-based sensor for visual nucleic acid detection.[126] After 10 min of RPA, SYBR green solution was added for double-strand nucleic acid staining. An increased fluorescence of the targeted DNA was detected under UV light, with is an excellent LOD of 10 copies μL^{-1} as well as a good selectivity (Figure 5D). Compared with other biomarkers, nucleic acid sensing can directly identify the pathogen species and even antibiotics-resistance genes. However, until today only a few studies have reported continuous quantifiable detection of nucleic acids. The precise controlling of the amplification rates and durations *in situ* is highly demanded. Furthermore, it is challenging to determine the spatial separation of polymerases and products, which is essential for continuous monitoring and downstream analysis. Further optimizations and combinations with other technologies such as nanopores and CRISPR systems are yet to be investigated.

3.3.3 Virulence factor sensors—Virulence factors such as enzymes and toxins secreted by bacteria are attractive infection biomarkers owing to their unique bioactivities. Figure 5E and 5F shows an infection sensor based on DNA hydrogel that can produce radio frequency change in response to deoxyribonuclease (DNase) secreted by pathogens.[127] The DNA hydrogel was designed by chemically crosslinked DNA strands that can be degraded by DNase and therefore modulated its capacitance. The capacity of infection sensing was then evaluated by applying the hydrogel on *Staphylococcus aureus*-infected wound in mice (Figure 5G). An increase of 0.4 V was observed after treating with 10^5 and 10^6 CFU for 24 h.

For example, *Pseudomonas aeruginosa* and *S. aureus*, two major bacteria species associated with chronic wounds, express α-hemolysin and phospholipase A_2 that can break down lipids.[130] Zhou and colleagues developed lipid vesicles with self-quenching dyes (Figure 5H).[128] Acetylenictricosadiynoic acids were employed for lipid stabilization in the aqueous environment to limit the vesicles' responsivity to virulence factors. As Figure 5I demonstrates, an elevated fluorescence density was observed in the presence of *P. aeruginosa* and *S. aureus*, but not in the non-toxic *Escherichia coli* group. A similar design can be also used for bacteria-responsive antibiotic delivery.[130–131] Another popular *P. aeruginosa*-secreted toxin biomarker is pyocyanin (PYO), which possesses redox-active properties.[132–133] Simoska et al. built carbon ultramicroelectrode arrays (CUAs) for PYO

identification by square wave voltammogram.[134] A detect range of 1–250 μM in simulated wound fluid was achieved, which covers the biologically relevant concentration (1–130 μM) of PYO.

3.4 Microorganism sensors

In addition to biomolecules, detecting microorganisms was also investigated for infection diagnosis. For example, Sheybani and Shukla developed a bacteria attachment sensor based on the resistance shifts upon bacteria colonization.[135] The sensor was able to perform an *in situ* electrochemical cleaning by applying a pulsed electric field to remove accumulated bacteria debris. The device was integrated with a metal oxide-based pH sensor and tested in simulated infected models *in vitro*. A LOD of 100 colony forming units (CFU) mL^{-1} was achieved. By using multiple sensor arrays, they could potentially provide continuous spatial infection information.

Utilizing biological recognition elements for bacterial sensing can also improve sensor selectivity. Aptasensors demonstrated in Figure 5A were capable of sensing *S. aureus* with a detection range of 0 to 1E+09 CFU mL^{-1}. Apart from aptamers, magainin-1, an antimicrobial peptide, was utilized by Dao and coworkers for bacteria detection.[136] Antimicrobial peptides naturally exist in numerous species as a part of the immune system. By covalent coating of magainin-1 on microfluidic chips, they achieved a LOD of 5 CFU mL^{-1} bacterial detection. Such bacterial enrichment designs can be potentially applied to electrochemical sensors by coupling them with redox agents. Antimicrobial peptides exhibit broad-spectrum selectivity with virus, gram-positive, and gram-negative bacteria. This eliminates the necessity of designing specific affinities for each infectious microorganism.

Recent progresses in wound biosensors have revealed the potential of using physical and biochemical signals for monitoring wound conditions. This can be also directly correlated to the newly identified biomarkers at wounds that are relevant with the healing process. However, there are still issues remaining to be addressed. One major challenge is to maintain the long-term stability of sensors since the chronic wound healing process may take months or even years. Also, the wound exudate volume is correlated with healing stage and can affect the concentration of some chemical analytes.[137–138] Therefore, real-time calibration of chemical sensing for accurate assessment is inevitable. Another issue is that current designs of wearable biosensors can only be applied for detecting a limited number of biomarkers. Numerous important biochemicals such nuclei acids, hormones, and immune cells still require off-body sampling for precisive analysis. Many emerging materials have been shown great potential in wound sensing such as 2D materials for enhanced sensitivity and stability of the sensors. In addition, wound fluid collection and *in situ* sampling can be greatly improved by newly developed fabrication techniques such as microfluidics patterns.[118, 139–143]

4. On-demand therapy

On-demand therapy systems are designed to actuate in response to specific physicochemical characteristics, which is a desirable property for dynamic chronic wound conditions. Both endogenous and exogenous responsive drug delivery systems (DDS) can promise

excellent functionality with less frequent patient intervention and reduced drug accumulation at off-target sites. Additionally, drug-free approaches such as electrical stimulation and thermodynamic therapy have been developed, showing promising healing potentials.

4.1 Responsive drug delivery systems (DDS)

4.1.1 Endogenously responsive DDS—Physical and biochemical pathological signals at chronic wounds can serve as stimuli for endogenous responsive systems. For example, Gao et al. designed a temperature-stimulated drug delivery patch based on the volume phase transition property of PNIPAM hydrogel.[144] When the wound temperature surpassed the lower critical solution temperature (LCST) of 37 °C, the hydrogel contracted and squeezed out the encapsulated drugs. Other thermo-responsive DDS based on biomaterials such as PNIPAM, Pluronics®, and poly(ethylene glycol) diacrylate (PEGDA) have been also developed with adjusted LCSTs of 36–40 °C for wound therapy.[162–163] However, the environment and individual temperature variations may prevent a precise control of thermoresponsive drug release.

Figure 6A presents an example of metabolite-responsive dressing for delivering insulin and fibroblasts for DFU management.[145] The hydrogel matrix was crosslinked with benzoic-imine bonds and phenylboronate esters, which are two widely used acidity- and glucose-sensitive designs, respectively.[164–166] In a diabetic rat wound model, the blood glucose level dropped from 474 to ~ 300 mg/dL and an accelerated healing process was observed after applying hydrogel dressings. However, due to the hydrophilic nature of hydrogels, they are not suitable for hydrophobic drug delivery. One possible solution could be encapsulating drug-loaded responsive and amphiphilic microparticles within the hydrogel matrix. For example, Hu et al. designed a pH and ROS-responsive wound dressing to reduce excessive inflammation (Figure 6B).[146] Amphiphilic micelles were prepared with ROS-degradable cholesterol-modified hyaluronic acid and encapsulated naproxen, a lipophilic anti-inflammatory drug. Next, boronic acids were grafted on the alginate backbone to form pH-sensitive hydrogel matrix, capable of entrapping antibiotics and the micelles. Antibacterial and anti-inflammation effects were further investigated in a *P. aeruginosa*-infected mice model. Apart from using metabolites as drug release triggers, protease-responsive DDS have been developed by direct conjugation of cargos into polymers with protease-cleavable linkers or entrapping into a protease-degradable matrix.[167–168]

However, loading capacities and drug releasing velocities in current designs often depend on the chemical properties of the polymeric scaffolds. In addition, long-term exposure to the wound microenvironment that contains various reactive chemicals may impair the stability and therapeutic activity of the loaded drugs.[169] To address these issues, Zhu et al. developed a mild encapsulation technology to entrap growth factors within polymer shells formed *in situ* (Figure 6C).[147] Monomers with different charges were non-covalently enriched around the growth factor molecules and formed nanocapsules with MMP-cleavable crosslinkers. A sequential release of vascular endothelial growth factor (VEGF) and platelet derived growth factor (PDGF) was obtained by employing the L or the D chiral forms of the crosslinker, respectively, to mimic the natural angiogenesis process

with maximum therapeutic efficiency.[170] This DDS enabled spatiotemporally controlled delivery of multiple drugs to promote wound healing.

4.1.2 Exogenously responsive DDS—Despite advances in DDS designs, drug release rates from endogenously responsive platforms are still primarily predetermined from the encapsulating matrices.[171] Furthermore, the physiological conditions may not change severely to enable efficient drug release at the early stage of infection. In comparison, exogenous signal triggered DDS that enable precise control of drug release dosing, timing, and location remotely, have been raising attention. Among those, wound dressings that are capable of responding to exogenous stimulus such as temperature, electric fields, and lights are the most common platforms. For example, a woven thermoresponsive wound patch was fabricated by Mostafalu et al. (Figure 7A).[148] They assembled carbon ink based conductive threads that could function as microheaters independently and coated with hydrogels encapsulating NIPAM/PEGDA particles as thermoresponsive drug carriers. By connecting the system to a microcontroller for wireless communication, they could raise the local temperature above the NIPAM/PEGDA system's critical temperature of 40 °C. The authors demonstrated antibacterial property and accelerated healing both *in vivo* and *in vitro* by the independently controllable release of VEGF and antibiotics from the textile patch.

In another strategy, as shown in Figure 7B, an electrical stimulated drug delivery wound patch was engineered to be capable of altering local pH electronically.[150] Positively charged drug loading-chitosan particles were encapsulated in PEGDA hydrogel with negatively charged laponite nanoparticles and covered at anodes. After applying an electrical field, the pH around the electrodes increased and impaired electrostatic interaction within the hydrogel matrix, leading to a drug release in a voltage-controlled manner. In addition, electronically controlled DDS can be coupled with electric stimulation therapy. Du et al. reported a triboelectric nanogenerator wound patch loaded with minocycline on the surface for antibacterial activity (Figure 7C).[161] As displayed in Figure 7D, electrical fields could impact drug release kinetics and allow a sufficient release. A synergistic effect was achieved by applying electrical fields and controlling minocycline release rate simultaneously in a *S. aureus* infected mice wound model.

Near-infrared (NIR) radiation provides another promising approach for exogenous controlled DDS. Light at wavelengths in the NIR region (650–900 nm) allows for deep penetration (hundreds of micrometers). NIR-responsive systems commonly incorporate nanomaterials for energy transduction. For example, Zhao et al. designed NIR-sensitive VEGF carriers using graphene oxides and PNIPAM due to their photothermal conversion and thermal responsive properties, respectively.[152] Beyond drug delivery, Figure 7E presents a NIR-mediated CO_2 generation for wound repair.[153] The proposed patch incorporated CuS nanoparticles for photothermal conversions and bicarbonate that could decompose into CO_2. CO_2 therapy could alleviate hypoxia by decreasing pH and inducing O_2 release from hemoglobin due to the Bohr effect. This CO_2 generating patch was advantageous over previous CO_2 gas delivery designs that require multiple injections.

However, the DDS loading capacity may restrict continuously O_2 or CO_2 production for gas-based wound therapies. To satisfy this requirement, Chen et al. designed an active wound

patch with a living cyanobacterium, *Synechococcus elongatus*, for O_2 and CO_2 generation via photosynthesis (Figure 7F and 7G).[154] A hydrophilic polytetrafluoroethylene (PTFE) membrane was used to prevent bacteria contaminations while allowing gas and water exchanges. Light-responsive gas production was demonstrated in Figure 7H. Notably, the authors reported a reversed hyperglycemia in response to O_2 level elevation owing to the decrease of HIF-1α expression. They also observed that the applied patch accelerated healing and achieved a wound closure time similar to normal wounds in diabetic wound models.

Current designs of DDS are responsive to various triggers and can potentially provide new therapeutic modalities due to their capability for on-demand and local drug release. However, there are some limitations that need to be addressed. First, most DDS are designed with confined drug amounts. Though incorporating living organisms may address this drawback, it is still facing longevity challenges due to difficulties in controlling bacterial on-patch viability. Secondly, few of the current designs could realize precise dosage control. For example, some hydrogel-based DDS response to a stimulus with a passive drug release that is driven by irreversible matrix breakdown. The administrated dosages mainly depend on the material degradation and are unrepeatable during a series of triggers. Further investigations in designing a rechargeable, stable, and controllable DDS are required for clinical translation.

4.2 Drug-free therapy

4.2.1 Electrical stimulation—It is estimated that an electrical field of 100–150 mV mm^{-1} occurs at cutaneous wounds naturally and guides the healing process including cell proliferation and migration via activating PI3K-Akt cell signaling pathways.[20, 172–173] Applying exogenous electrical fields exhibits therapeutic effects in a biomimicking way with minimal adverse effects. Currently, both high-voltage pulsed (clinically 75–150 V with <50 μs phase durations and >100 pps frequency) and low-voltage (<50 V) devices have been developed for clinical usage.[174]

An electrical stimulation device was designed by Wang et al. for delivering high-voltage monophase pulsed currents to accelerate wound healing (Figure 8A).[156] Commercial Chitosan-Vaseline gauze was integrated for moisture retention and antibacterial function. The device was then connected to an isolated pulse stimulator for electrical current supply, resulting in high therapeutic efficiency *in vivo*. In another study, Ershad et al. reported a drawn-on-skin (DoS) electronics platform for low-voltage electrical stimulation wound therapy (Figure 8B and 8C).[157] A conductive ink was formulated with Ag flakes and poly(3,4-ethylenedioxythiophene)-poly(styrenesulfonate) (PEDOT:PSS) and directly patterned on the skin with a tape stencil. Using this platform, they were able to directly draw the electronics on the wound site in a mice model. By connecting with a DC stimulator, they observed an accelerated healing process. Such a DoS platform could enable on-the-go wound management with customized shapes and sizes.

In general, high-voltage based therapy needs large extracorporeal devices with controlled frequency and pulse width to avoid tissue damage caused by long-term stimulations. Additionally, the high voltage could damage some biomaterials-based electrodes.

Comparatively, it is simpler to generate low-voltage electrical stimulation wirelessly on wearable devices. For example, Figure 8D displays a flexible bandage generating low-voltage electrical fields from a miniatured wearable nanogenerator.[158] After wrapping rats with the bandages, the nanogenerators could output pulsed electrical fields by converting breath-caused body motions (Figure 8E). A maximum voltage of around 2.2 V was achieved at an active status of the rat. The wound healing efficiency was demonstrated in Figure 8F with the healing time reducing from 12 to 3 days. However, this design required a regular body displacement pattern to generate uniform electrical fields. Further modifications are necessary when it is applied for human wounds on arms or limbs.

4.2.2 Photodynamic therapy—Another emerging drug-free approach for wound management is photodynamic therapy. In this technique, light and photosensitizers are used to generate ROS and kill multi-drug resistant bacteria. Nanostructured titanium dioxide (TiO_2) and zinc oxide (ZnO), with similar bandgap energy of ~ 3.2 eV, are two well-known materials with photosensitizing properties.

Yu and coworkers assembled a TiO_2-based nanorod array by incorporating $BaTiO_3$ and gold nanoparticles (Au NPs) (Figure 8G).[159] Under light illumination, Au NPs could produce hot electrons and transfer them to TiO_2, enhancing ROS generation; while ferroelectric properties of $BaTiO_3$ were deduced to further enhance the electrons' mobility via a piezophototronic effect. It was observed that with a positive poling, the co-axis TiO_2/$BaTiO_3$/Au could generate 2.8-folds of •OH and 4-folds of $^1O_2$ when compared to those generated by groups formulated without $BaTiO_3$ or Au. Antibacterial efficiency of > 99% was achieved against both *E. coli* and *S. aureus* after 40 min simulated sunlight exposure. Another strategy has embedded ZnO as photosensitizer and Ag/Ag@AgCl to improve the photocatalytic performance within the hydrogel matrix for wound therapy (Figure 8H).[160] In addition, the antibacterial properties of Ag^+ and fibroblast proliferative capability of Zn^{2+} could have synergistic effects in the healing process. As Figure 8I shows, the synthesized hydrogel exhibited bacterial disinfection in a light-responsive behavior. Although the *in vitro* study showed a slightly higher antibacterial function of Ag/Ag@AgCl over the Ag/Ag@AgCl/ZnO hydrogel, the introduced ZnO contributed to a better healing process in a mice model.

The photodynamic process can be regulated by factors such as light exposure dose, oxygen level, and photosensitizers' photocatalytic activities. In addition, the short half-life of the ROS allows localized bacterial damage with minimal tissue toxicity.[175] Advances in optimizing photoenergy conversion efficiency and improving the biocompatibility of devices would encompass the applicability in wound management.

Recent advances in on-demand wound treatment methods have opened new windows in developing versatile therapeutic platforms by using wounds closed loop systems. Despite the controllable feature of on-demand therapy systems, there are still challenges to be addressed for broad applicability. One major concern is the longevity challenges of DDS. Though some commercial sustainable drug release systems can maintain their efficacy for months or even years, only a few of the available systems can function for on-demand drug delivery.[176] In addition, due to the complex nature of wound microenvironment, involving various

biochemical reactions and cell interactions, the healing process may not be efficiently accelerated by administrating one or two types of treatments. For example, electric stimulation therapy provided a biomimicking way to promote cell migration and fibroblast differentiation with minimal reverse effects. Its efficiency has been observed in many clinical trials while it could not provide personalized therapy such as immunomodulation and preventing infection. Detailed discussions about therapeutic methods are listed in Table 1. Another promising approach is the delivery of genetic drugs or programmable cells to control skin cells behavior and improve tissue regeneration with durable clinical responses. Recent advances in tissue transfection and cell therapy could benefit personalized wound healing in the future.[177–178]

5. Integrated closed loop systems

Over the past decades, fully functioning systems have been developed underlying various technologies to fulfill the purpose of chronic wound management. Self-powered wireless platforms are capable of improving patient adherence and therapeutic efficacy. In addition, advanced data analysis and interpretation tools are required to process large information harvested from bioelectronics. In this section, we introduce wireless integrated wearable wound bioelectronics and highlight AI applications for personalized wound management.

5.1 Self-powered designs

Long-term sensing and controllable therapy require sustainable power supplies. To achieve this goal, self-powered bioelectronics are designed by harvesting different energy sources and converting them into electricity.[179–180]

Harvesting energy from biomechanical motions such as walking, breathing, and limb movements is one promising strategy. It is estimated that electrical energy generated from typical human motions could reach up to 39 W.[181] Figure 9A shows a piezoelectric dermal patch composed of ZnO nanorod and sandwiched by PDMS. By applying a uniform mechanical stress along the y-axis of the ZnO nanorod, the authors theoretically demonstrated that a polarized charge distribution and potential would be generated (Figure 9B). The *in vivo* piezoelectric voltage generation in a mice wound model showed electrical pulses with an average 900-mV amplitude and a 200-ms pulse width (Figure 9C). A similar design using triboelectric nanogenerators for electrical stimulation wound therapy was mentioned earlier.[158]

The confluent metabolites in the wound are recognized as another appealing energy source. In Figure 9D, a biofuel cell (BFC)-powered electrochromic timer was developed to record the duration of drug administration.[183] The upper layer of the flexible patch was built with a PEDOT/polyurethane (PU) film and a fructose dehydrogenase (FDH)-coated carbon electrode. This layer could be activated by interstitial fluid-mediated connection with the bottom fructose-containing hydrogel layer. The fructose redox reaction enabled color change of PEDOT/PU film, acting as a function of electrical potential and time course (Figure 9E). In addition, many BFC-based bioelectronic devices have been developed and integrated with metabolic sensors, which could also be potentially applied for wound management. [109, 185–186]

Apart from directly harvesting energy from the human body, recent technologies in near-field communication (NFC) enable wireless power supplies. Krishnan et al. reported an NFC-based dermal patch for both wireless physical signal measurements and data transmission (Figure 9F and 9G).[184] The prepared patch was applied on human burn wounds and allowed a direct smartphone readout.

5.2 Integrated closed-loop systems

Closed loop wearable wound bioelectronics typically contain four fundamental components:1) biosensors for collecting wound condition parameters; 2) algorithms for analyzing input signals and issuing desired intervention commands; 3) controllable therapeutics systems; and 4) wireless communication modules for data transmission. For example, a closed-loop patch was engineered for wound pH and temperature monitoring as well as a microheater-controlled thermo-responsive drug release system (Figure 10A and 10B).[149] In addition, a Bluetooth module was integrated with the system for wireless sensor readouts and microheater control. The patch performance was further evaluated in a bioreactor that mimicked *in vivo* bacterial growth. As shown in Figure 10C, the bandage was automatically activated and released antibiotics when the pH was reduced to a predetermined threshold value. However, the temperature increase as a result of wound infection could interfere with the thermo-responsive drug release process. To address this issue, Pang et al. chose ultraviolet (UV) as a separate exogenous stimulus to regulate the drug release and integrated with wound temperature sensors (Figure 10D and 10E).[155] UV light-emitting diodes (UV-LED) were implemented to control the bottom UV-cleavable antibiotics-loaded hydrogel layer. The whole device was connected to a Bluetooth module and applied to an infected wound model in pigs. The results showed that the UV irradiation was activated to operate the drug delivery actuators when wound temperature exceeded the safe limit value (Figure 10F). In addition to single parameter-based regulation, a closed loop wound management device that could record pH, temperature, and UA levels to control the drug release electronically was built (Figure 10G and 10H).[151] As illustrated in Figure 10I, the device could transfer data wirelessly between the smartphone and rat through NFC technology. The authors also reported that all of the three signals displayed significant deviations from physiological ranges in infected wound models, suggesting the device's potential in reducing the false positive diagnosis rate by combining different biomarkers.

5.3 Artificial intelligence (AI)

The actuation of most current closed loop systems is regulated by rule-based algorithms and largely depends on defined values. To improve therapeutic efficacy, an advanced closed loop system is required to incorporate various biomarkers' information and operate a comprehensive analysis. In addition, the system must be capable of managing different wound milieus such as potential antibiotics resistance of different bacterial species, changes in drug potency at certain pH and temperature, glucose variations in DFU, and patient-specific underlying health conditions. Recent developments of various training methodologies (e.g. artificial neural network (ANN), instance-based algorithms, decision tree algorithms) in AI are promising tools to process a large amount of patient-centered databases, discovering certain trends and therapeutic opportunities, and drawing actionable and valuable conclusions for personalized intervention (Figure 11).[20, 187–189]

Recently, machine learning algorithms have shown great promise for wound image processing to identify wound features and pathological signals. Both two-dimensional (2D) images and 3D wound modeling systems are developed to accurately measure wound parameters such as color, area, and volume in a non-invasive way.[188] These technologies are useful for further AI-based image processing for wound classification and assessment. For example, Veredas et al. constructed a machine learning assisted system for pressure ulcer image segment and classification.[190] They evaluated the performance of ANN, support vector machines (SVM) and random forest (RF) decision trees in identifying wound-bed conditions such as necrotic, slough, healing, granulation and peri-ulcer skin tissue. All three machine learning approaches achieved excellent accuracy (>85%).

Infection management is another application of AI implemented wound therapy. Ward and colleagues implemented AI in bioelectronics to mitigate antibiotic side effects. They developed a closed loop wound patch integrated with a PYO sensor, ANN-assisted antibiotics toxicity prediction, and controllable dosing modules.[191] A series of studies in AI algorithms such as prediction of sepsis, hospital-acquired infections, antibiotics resistance were also conducted, which could be useful for chronic wound care.[189, 192]

In summary, AI provides data-driven approaches to facilitate wound management. However, establishing consistent and robust AI implemented closed loop systems requires further training and verifying in complex and diverse clinical samples.

To this end, a growing number of integrated devices have emerged in the form of wearable bioelectronics for closed loop wound care. Recent breakthroughs in biomaterial science and digital health intervention promise to precisely control wound treatment in response to the physiological information collected by wound sensors. In addition, the implementation of AI can help identify certain recurrent patterns and potentially accelerate the decision-making process by choosing personalized therapeutic methods and predicting optimized dosing amount for patients. However, some challenges are still remaining. For example, most stimuli responsive DDS in integrated systems are based on one or two signal changes at the wounds. Moreover, integrating multiplexed biosensors and treatment methods in the same patch while controlling the drug administration with minimal crosstalk and interferences is a tremendous challenge. Further improvement of sensor selectivity and deployment of different types of sensors (i.e., enzymatic sensors, ionic selective sensors, impedance-based sensors, etc.) may solve this problem. Furthermore, a better understanding of types, dosing amount, and duration of drug administration in relation to various analytes in wound exudates and healing process is still required.

6. Conclusions and outlook

Wearable bioelectronics holds great potential to surmount many challenges in wound management, particularly in increasing patient adherence and providing new modes of chronic wound therapy. In summary, we have reviewed and highlighted recent advances in wearable biosensors for comprehensive wound condition assessments via a list of physical, small molecular, macromolecular, and microorganism biomarkers, as well as on-demand therapeutic system designs. The new generation of closed loop wearable wound

bioelectronics is capable of fast and noninvasive detection of biomarkers as well as dynamic and automated therapeutic administration. These advances in integrated systems have attracted significant research interest due to their advantages in reducing patient intervention and enhancing therapeutic efficiency. Furthermore, considering the development of multiplexed wound biosensors, implementing advanced data analysis algorithms could contribute to a large amount of data processing. By applying machine learning technologies, next-generation wearable bioelectronics would be able to generate data-based clinical decisions and reliable predictions, expanding their applicability and functionality in personalized wound care.

However, there are still several bottlenecks remaining to be addressed in future works in the wound care area. For example, one major issue of biosensors is that they require a certain amount of wound fluid in order to function properly. However, efficient collecting of wound fluid *in situ* is a challenge. In addition, the inability to control wound fluid generation and collection rate may also lead to inconsistent sample concentration and signal unreliability. Recently, most wearable devices only tested small molecular biomarker monitoring *in vitro* using simulated wound fluids without wound fluid collection designs. Particularly, only handful of wound bioelectronic devices were tested to detect comprehensive biochemical signals *in vivo*. Advanced engineering approaches such as microfluidics channels and microneedle arrays as well as novel materials should be implemented to enable efficient wound fluid collection in a controllable manner.

Another challenge is to achieve continuous monitoring of a broad spectrum of biomarkers with on-device processing. Most current available devices can only continuously monitor a limited number of targets such as physical signals (e.g., pressure, temperature) and several common analytes (e.g. glucose, uric acid). While wound involves many detectable levels of proteins, enzymes, and lipids that could benefit early detection of pathological conditions, only few current designs were capable of continuous detection of these biomarkers and overcome longevity challenges. Future wound bioelectronics should integrate novel biotechnologies and materials chemistry to expand on-device detectable biomarkers and enable long-term monitoring with minimal on-site sample preparations. Moreover, further understanding and clinical evaluation of these biomarkers' relevance to the healing process and prognosis is also necessary to improve biosensor designs and therapeutic applications.

In addition, deploying engineering approaches in fabrication such as bioprinting, lithography, laser cutting, and robot forming promises to enable scalable production with customized architectures. Last but not least, considering that most effort has been invested in the technology development and evaluation at the bench side or on animal models, the validation and utility of the wearable bioelectronic devices on human subjects need to be carefully investigated following proper ethical guidelines.[193] Future devices envision to be capable of providing off-the-shelf solutions for emergent conditions such as wounded troops on the battlefield as well as affordable in-home wound therapy for patients in rural areas. In the foreseeable future, highly integrated wound management systems with outstanding wearability, diverse functionality, and excellent longevity will be developed and facilitated by AI to revolutionize personalized wound care.

Acknowledgements

This project was supported by the National Institutes of Health grant R01HL155815, Office of Naval Research grants N00014-21-1-2483 and N00014-21-1-2845, the Translational Research Institute for Space Health through NASA NNX16AO69A, and Rothenberg Innovation Initiative (RI^2) and Rosen Center for Bioengineering at California Institute of Technology.

Biography

Canran Wang received a B.S. degree in biomedical sciences from Shanghai Jiao Tong University. She joined Dr. Wei Gao's research group in 2021, pursuing her Ph.D. degree in medical engineering at Caltech. Her current research interests include wearable biosensors and wound healing.

Ehsan Shirzaei Sani received his Ph.D. in chemical engineering from the University of California, Los Angeles in 2020. He is currently a postdoctoral research associate in medical engineering at the California Institute of Technology. His current research focuses on design and development of smart wearable bioelectronics for disease monitoring, diagnosis, and treatment.

Wei Gao is currently an assistant professor of medical engineering at the California Institute of Technology. He received his Ph.D. in chemical engineering from the University of California, San Diego in 2014. He worked as a postdoctoral fellow in electrical engineering and computer sciences at the University of California, Berkeley between 2014 and 2017. His current research interests include wearable biosensors, robotics, flexible electronics, and nanomedicine.

References:

[1]. Li D, Kular L, Vij M, Herter EK, Li X, Wang A, Chu T, Toma MA, Zhang L, Liapi E, Mota A, Blomqvist L, Gallais Sérézal I, Rollman O, Wikstrom JD, Bienko M, Berglund D, Ståhle M, Sommar P, Jagodic M, Landén NX, Proceedings of the National Academy of Sciences of the United States of America 2019, 116, 9443. [PubMed: 31019085]

[2]. McLister A, McHugh J, Cundell J, Davis J, Advanced Materials 2016, 28, 5732. [PubMed: 26821765]

[3]. Sen CK, Gordillo GM, Roy S, Kirsner R, Lambert L, Hunt TK, Gottrup F, Gurtner GC, Longaker MT, Wound Repair Regen 2009, 17, 763. [PubMed: 19903300]

[4]. Derakhshandeh H, Kashaf SS, Aghabaglou F, Ghanavati IO, Tamayol A, Trends Biotechnol 2018, 36, 1259. [PubMed: 30197225]

[5]. Zhang A, Lieber CM, Chemical Reviews 2016, 116, 215. [PubMed: 26691648]

[6]. Park S, Kang YJ, Majd S, Advanced Materials 2015, 27, 7583. [PubMed: 26397962]

[7]. Piccolino M, Trends in Neurosciences 2000, 23, 147. [PubMed: 10717671]

[8]. Xu C, Yang Y, Gao W, Matter 2020, 2, 1414. [PubMed: 32510052]

[9]. Kringelbach ML, Jenkinson N, Owen SL, Aziz TZ, Nature reviews. Neuroscience 2007, 8, 623. [PubMed: 17637800]

[10]. Gutruf P, Yin RT, Lee KB, Ausra J, Brennan JA, Qiao Y, Xie Z, Peralta R, Talarico O, Murillo A, Chen SW, Leshock JP, Haney CR, Waters EA, Zhang C, Luan H, Huang Y, Trachiotis G, Efimov IR, Rogers JA, Nature Communications 2019, 10, 5742.

[11]. Zeng W, Shu L, Li Q, Chen S, Wang F, Tao X-M, Advanced Materials 2014, 26, 5310. [PubMed: 24943999]

[12]. Kim DH, Lu N, Ma R, Kim YS, Kim RH, Wang S, Wu J, Won SM, Tao H, Islam A, Yu KJ, Kim TI, Chowdhury R, Ying M, Xu L, Li M, Chung HJ, Keum H, McCormick M, Liu P, Zhang YW, Omenetto FG, Huang Y, Coleman T, Rogers JA, Science 2011, 333, 838. [PubMed: 21836009]

[13]. Gao W, Emaminejad S, Nyein HYY, Challa S, Chen K, Peck A, Fahad HM, Ota H, Shiraki H, Kiriya D, Lien DH, Brooks GA, Davis RW, Javey A, Nature 2016, 529, 509. [PubMed: 26819044]

[14]. Someya T, Bao Z, Malliaras GG, Nature 2016, 540, 379. [PubMed: 27974769]

[15]. Kim J, Campbell AS, de Avila BE, Wang J, Nat Biotechnol 2019, 37, 389. [PubMed: 30804534]

[16]. Moffatt C, Murray S, Keeley V, Aubeeluck A, International Wound Journal 2017, 14, 1305. [PubMed: 28857457]

[17]. Yang Y, Gao W, Chemical Society Reviews 2019, 48, 1465. [PubMed: 29611861]

[18]. Choi S, Lee H, Ghaffari R, Hyeon T, Kim D-H, Advanced Materials 2016, 28, 4203. [PubMed: 26779680]

[19]. Zhou X, Qu M, Tebon P, Jiang X, Wang C, Xue Y, Zhu J, Zhang S, Oklu R, Sengupta S, Sun W, Khademhosseini A, Advanced Science 2020, 7, 2001447. [PubMed: 33042756]

[20]. Zajdel TJ, Shim G, Wang L, Rossello-Martinez A, Cohen DJ, Cell Systems 2020, 10, 506. [PubMed: 32684277]

[21]. Feiner R, Dvir T, Nature Reviews Materials 2017, 3, 17076.

[22]. Schiavone G, Lacour SP, Science translational medicine 2019, 11.

[23]. Schneider LA, Korber A, Grabbe S, Dissemond J, Archives of Dermatological Research 2007, 298, 413. [PubMed: 17091276]

[24]. Mouthuy P-A, Snelling SJB, Dakin SG, Milković L, Gašparović AČ, Carr AJ, Žarković N, Biomaterials 2016, 109, 55. [PubMed: 27669498]

[25]. Patruno A, Ferrone A, Costantini E, Franceschelli S, Pesce M, Speranza L, Amerio P, D'Angelo C, Felaco M, Grilli A, Reale M, Cell proliferation 2018, 51, e12432. [PubMed: 29357406]

[26]. Sala de Medeiros M, Chanci D, Moreno C, Goswami D, Martinez RV, Advanced Functional Materials 2019, 29, 1904350.

[27]. Xia D-L, Chen Y-P, Wang Y-F, Li X-D, Bao N, He H, Gu H-Y, Advances in Skin & Wound Care 2016, 29.

[28]. Tehrani-Bagha AR, Advances in Colloid and Interface Science 2019, 268, 114. [PubMed: 31022590]

[29]. Peng X, Dong K, Ye C, Jiang Y, Zhai S, Cheng R, Liu D, Gao X, Wang J, Wang ZL, Science Advances 2020, 6, eaba9624. [PubMed: 32637619]

[30]. Guan X, Xu B, Wu M, Jing T, Yang Y, Gao Y, Nano Energy 2021, 80, 105549.

[31]. Shi L, Liu X, Wang W, Jiang L, Wang S, Advanced Materials 2019, 31, 1804187.

[32]. Lao L, Shou D, Wu YS, Fan JT, Science Advances 2020, 6, eaaz0013. [PubMed: 32284976]

[33]. Klopfleisch R, Jung F, Journal of Biomedical Materials Research Part A 2017, 105, 927. [PubMed: 27813288]

[34]. Anderson JM, Rodriguez A, Chang DT, Semin Immunol 2008, 20, 86. [PubMed: 18162407]

[35]. Brodbeck WG, Patel J, Voskerician G, Christenson E, Shive MS, Nakayama Y, Matsuda T, Ziats NP, Anderson JM, Proceedings of the National Academy of Sciences 2002, 99, 10287.

[36]. Salatino JW, Ludwig KA, Kozai TDY, Purcell EK, Nature Biomedical Engineering 2017, 1, 862.

[37]. Santamaría B, Ucero AC, Benito-Martin A, Vicent MJ, Orzáez M, Celdrán A, Selgas R, Ruíz-Ortega M, Ortiz A, Blood purification 2015, 39, 200. [PubMed: 25765663]

[38]. Mu Q, Yang L, Davis JC, Vankayala R, Hwang KC, Zhao J, Yan B, Biomaterials 2010, 31, 5083. [PubMed: 20378165]

[39]. Griffin DR, Archang MM, Kuan C-H, Weaver WM, Weinstein JS, Feng AC, Ruccia A, Sideris E, Ragkousis V, Koh J, Plikus MV, Di Carlo D, Segura T, Scumpia PO, Nature Materials 2021, 20, 560. [PubMed: 33168979]

[40]. Ito M, Yang Z, Andl T, Cui C, Kim N, Millar SE, Cotsarelis G, Nature 2007, 447, 316. [PubMed: 17507982]

[41]. Wynn TA, Vannella KM, Immunity 2016, 44, 450. [PubMed: 26982353]

[42]. Jin SS, He DQ, Luo D, Wang Y, Yu M, Guan B, Fu Y, Li ZX, Zhang T, Zhou YH, Wang CY, Liu Y, ACS Nano 2019, 13, 6581. [PubMed: 31125522]

[43]. Zahouani H, Pailler-Mattei C, Sohm B, Vargiolu R, Cenizo V, Debret R, Skin research and technology : official journal of International Society for Bioengineering and the Skin (ISBS) [and] International Society for Digital Imaging of Skin (ISDIS) [and] International Society for Skin Imaging (ISSI) 2009, 15, 68.

[44]. Guimarães CF, Gasperini L, Marques AP, Reis RL, Nature Reviews Materials 2020, 5, 351.

[45]. Vining KH, Mooney DJ, Nature Reviews Molecular Cell Biology 2017, 18, 728. [PubMed: 29115301]

[46]. Chu S-Y, Chou C-H, Huang H-D, Yen M-H, Hong H-C, Chao P-H, Wang Y-H, Chen P-Y, Nian S-X, Chen Y-R, Liou L-Y, Liu Y-C, Chen H-M, Lin F-M, Chang Y-T, Chen C-C, Lee OK, Nature Communications 2019, 10, 1524.

[47]. Yang H, Nguyen KT, Leong DT, Tan NS, Tay CY, ACS Applied Materials & Interfaces 2016, 8, 26591. [PubMed: 27608498]

[48]. Lacour SP, Courtine G, Guck J, Nature Reviews Materials 2016, 1, 16063.

[49]. Yuk H, Lu B, Zhao X, Chemical Society Reviews 2019, 48, 1642. [PubMed: 30474663]

[50]. Feig VR, Tran H, Lee M, Bao Z, Nature Communications 2018, 9, 2740.

[51]. Gozen BA, Tabatabai A, Ozdoganlar OB, Majidi C, Advanced Materials 2014, 26, 5211. [PubMed: 24899382]

[52]. Kim D-H, Lu N, Ma R, Kim Y-S, Kim R-H, Wang S, Wu J, Won SM, Tao H, Islam A, Yu KJ, Kim T.-i., Chowdhury R, Ying M, Xu L, Li M, Chung H-J, Keum H, McCormick M, Liu P, Zhang Y-W, Omenetto FG, Huang Y, Coleman T, Rogers JA, Science 2011, 333, 838. [PubMed: 21836009]

[53]. Xu S, Yan Z, Jang K-I, Huang W, Fu H, Kim J, Wei Z, Flavin M, McCracken J, Wang R, Badea A, Liu Y, Xiao D, Zhou G, Lee J, Chung HU, Cheng H, Ren W, Banks A, Li X, Paik U, Nuzzo RG, Huang Y, Zhang Y, Rogers JA, Science 2015, 347, 154. [PubMed: 25574018]

[54]. Yuk H, Varela CE, Nabzdyk CS, Mao X, Padera RF, Roche ET, Zhao X, Nature 2019, 575, 169. [PubMed: 31666696]

[55]. Yang J, Bai R, Chen B, Suo Z, Advanced Functional Materials 2020, 30, 1901693.

[56]. Nam S, Mooney D, Chemical Reviews 2021, DOI: 10.1021/acs.chemrev.0c00798.

[57]. Chen J, Wang D, Wang L-H, Liu W, Chiu A, Shariati K, Liu Q, Wang X, Zhong Z, Webb J, Schwartz RE, Bouklas N, Ma M, Advanced Materials 2020, 32, 2001628.

[58]. Li J, Celiz AD, Yang J, Yang Q, Wamala I, Whyte W, Seo BR, Vasilyev NV, Vlassak JJ, Suo Z, Mooney DJ, Science 2017, 357, 378. [PubMed: 28751604]

[59]. Blacklow SO, Li J, Freedman BR, Zeidi M, Chen C, Mooney DJ, Science Advances 2019, 5, eaaw3963. [PubMed: 31355332]

[60]. Shagan A, Zhang W, Mehta M, Levi S, Kohane DS, Mizrahi B, Advanced Functional Materials 2020, 30, 1900998.

[61]. Deng J, Yuk H, Wu J, Varela CE, Chen X, Roche ET, Guo CF, Zhao X, Nature Materials 2021, 20, 229. [PubMed: 32989277]

[62]. Wang D-A, Varghese S, Sharma B, Strehin I, Fermanian S, Gorham J, Fairbrother DH, Cascio B, Elisseeff JH, Nature Materials 2007, 6, 385. [PubMed: 17435762]

[63]. Hodinka RL, Journal of clinical microbiology 2013, 51, 2. [PubMed: 23052302]

[64]. Gardner SE, Frantz RA, Doebbeling BN, Wound Repair and Regeneration 2001, 9, 178. [PubMed: 11472613]

[65]. Webb RC, Bonifas AP, Behnaz A, Zhang Y, Yu KJ, Cheng H, Shi M, Bian Z, Liu Z, Kim Y-S, Yeo W-H, Park JS, Song J, Li Y, Huang Y, Gorbach AM, Rogers JA, Nature Materials 2013, 12, 938. [PubMed: 24037122]

[66]. Jeon J, Lee H-B-R, Bao Z, Advanced Materials 2013, 25, 850. [PubMed: 23233317]

[67]. Fromme NP, Li Y, Camenzind M, Toncelli C, Rossi RM, Advanced Electronic Materials 2021, 7, 2001238.

[68]. Wang C, Xia K, Wang H, Liang X, Yin Z, Zhang Y, Advanced Materials 2019, 31, 1801072.

[69]. Kim D-H, Wang S, Keum H, Ghaffari R, Kim Y-S, Tao H, Panilaitis B, Li M, Kang Z, Omenetto F, Huang Y, Rogers JA, Small 2012, 8, 3263. [PubMed: 22893603]

[70]. Sharifuzzaman M, Chhetry A, Zahed MA, Yoon SH, Park CI, Zhang S, Chandra Barman S, Sharma S, Yoon H, Park JY, Biosensors and Bioelectronics 2020, 169, 112637. [PubMed: 33007617]

[71]. Yang Y, Song Y, Bo X, Min J, Pak OS, Zhu L, Wang M, Tu J, Kogan A, Zhang H, Hsiai TK, Li Z, Gao W, Nature Biotechnology 2020, 38, 217.

[72]. Lou D, Pang Q, Pei X, Dong S, Li S, Tan W.-q., Ma L, Biosensors and Bioelectronics 2020, 162, 112275. [PubMed: 32392156]

[73]. Swisher SL, Lin MC, Liao A, Leeflang EJ, Khan Y, Pavinatto FJ, Mann K, Naujokas A, Young D, Roy S, Harrison MR, Arias AC, Subramanian V, Maharbiz MM, Nature Communications 2015, 6, 6575.

[74]. Kalidasan V, Yang X, Xiong Z, Li RR, Yao H, Godaba H, Obuobi S, Singh P, Guan X, Tian X, Kurt SA, Li Z, Mukherjee D, Rajarethinam R, Chong CS, Wang J-W, Ee PLR, Loke W, Tee BCK, Ouyang J, Charles CJ, Ho JS, Nature Biomedical Engineering 2021, 5, 1217.

[75]. Tao J, Dong M, Li L, Wang C, Li J, Liu Y, Bao R, Pan C, Microsystems & Nanoengineering 2020, 6, 62. [PubMed: 34567673]

[76]. Gao L, Zhang Y, Malyarchuk V, Jia L, Jang K-I, Chad Webb R, Fu H, Shi Y, Zhou G, Shi L, Shah D, Huang X, Xu B, Yu C, Huang Y, Rogers JA, Nature Communications 2014, 5, 4938.

[77]. Najafabadi AH, Tamayol A, Annabi N, Ochoa M, Mostafalu P, Akbari M, Nikkhah M, Rahimi R, Dokmeci MR, Sonkusale S, Ziaie B, Khademhosseini A, Advanced Materials 2014, 26, 5823. [PubMed: 25044366]

[78]. Sen CK, Gordillo GM, Roy S, Kirsner R, Lambert L, Hunt TK, Gottrup F, Gurtner GC, Longaker MT, Wound Repair Regen. 2009, 17, 763. [PubMed: 19903300]

[79]. Matsukawa R, Miyamoto A, Yokota T, Someya T, Advanced Healthcare Materials 2020, 9, 2001322.

[80]. Wei M, Zhang Y, Li G, Ni Y, Wang S, Zhang F, Zhang R, Yang N, Shao S, Wang P, Biosensors & bioelectronics 2019, 124–125, 25.

[81]. Cui Y, An Y, Jin T, Zhang F, He P, Sensors and Actuators B: Chemical 2017, 250, 461.

[82]. Pei X, Jin H, Dong S, Lou D, Ma L, Wang X, Cheng W, Wong H, Vacuum 2019, 168, 108808.

[83]. Armstrong DG, Boulton AJM, Bus SA, The New England journal of medicine 2017, 376, 2367. [PubMed: 28614678]

[84]. Bus SA, Armstrong DG, van Deursen RW, Lewis JE, Caravaggi CF, Cavanagh PR, Diabetes/metabolism research and reviews 2016, 32 Suppl 1, 25. [PubMed: 26813614]

[85]. Mishra RB, El-Atab N, Hussain AM, Hussain MM, Advanced Materials Technologies 2021, 6, 2001023.

[86]. Tao L-Q, Zhang K-N, Tian H, Liu Y, Wang D-Y, Chen Y-Q, Yang Y, Ren T-L, ACS Nano 2017, 11, 8790. [PubMed: 28800221]

[87]. Jian M, Xia K, Wang Q, Yin Z, Wang H, Wang C, Xie H, Zhang M, Zhang Y, Advanced Functional Materials 2017, 27, 1606066.

[88]. Wu Q, Qiao Y, Guo R, Naveed S, Hirtz T, Li X, Fu Y, Wei Y, Deng G, Yang Y, Wu X, Ren T-L, ACS Nano 2020, 14, 10104. [PubMed: 32667779]

[89]. Abbott CA, Chatwin KE, Foden P, Hasan AN, Sange C, Rajbhandari SM, Reddy PN, Vileikyte L, Bowling FL, Boulton AJM, Reeves ND, The Lancet Digital Health 2019, 1, e308. [PubMed: 33323253]

[90]. Jones EM, Cochrane CA, Percival SL, Adv Wound Care (New Rochelle) 2015, 4, 431. [PubMed: 26155386]

[91]. Guinovart T, Valdés-Ramírez G, Windmiller JR, Andrade FJ, Wang J, Electroanalysis 2014, 26, 1345.

[92]. Rahimi R, Ochoa M, Tamayol A, Khalili S, Khademhosseini A, Ziaie B, ACS Applied Materials & Interfaces 2017, 9, 9015. [PubMed: 28224783]

[93]. Pal A, Goswami D, Cuellar HE, Castro B, Kuang S, Martinez RV, Biosensors and Bioelectronics 2018, 117, 696. [PubMed: 30014943]

[94]. Huang W-D, Cao H, Deb S, Chiao M, Chiao JC, Sensors and Actuators A: Physical 2011, 169, 1.

[95]. Koh A, Kang D, Xue Y, Lee S, Pielak RM, Kim J, Hwang T, Min S, Banks A, Bastien P, Manco MC, Wang L, Ammann KR, Jang K-I, Won P, Han S, Ghaffari R, Paik U, Slepian MJ, Balooch G, Huang Y, Rogers JA, Science translational medicine 2016, 8, 366ra165.

[96]. Zhu Y, Zhang J, Song J, Yang J, Du Z, Zhao W, Guo H, Wen C, Li Q, Sui X, Zhang L, Advanced Functional Materials 2020, 30, 1905493.

[97]. Ochoa M, Rahimi R, Zhou J, Jiang H, Yoon CK, Maddipatla D, Narakathu BB, Jain V, Oscai MM, Morken TJ, Oliveira RH, Campana GL, Cummings OW, Zieger MA, Sood R, Atashbar MZ, Ziaie B, Microsystems & Nanoengineering 2020, 6, 46. [PubMed: 34567658]

[98]. Kassal P, Kim J, Kumar R, de Araujo WR, Steinberg IM, Steinberg MD, Wang J, Electrochemistry Communications 2015, 56, 6.

[99]. Nery RA, Skare TL, An Bras Dermatol 2019, 94, 369. [PubMed: 31365675]

[100]. Sharp D, Davis J, Electrochemistry Communications 2008, 10, 709.

[101]. Castilla DM, Liu Z-J, Velazquez OC, Adv Wound Care (New Rochelle) 2012, 1, 225. [PubMed: 24527310]

[102]. Sen CK, Wound Repair and Regeneration 2009, 17, 1. [PubMed: 19152646]

[103]. Arsenault KA, McDonald J, Devereaux PJ, Thorlund K, Tittley JG, Whitlock RP, Wound Repair and Regeneration 2011, 19, 657. [PubMed: 22092835]

[104]. Ruangsetakit C, Chinsakchai K, Mahawongkajit P, Wongwanit C, Mutirangura P, Journal of Wound Care 2010, 19, 202. [PubMed: 20505593]

[105]. Marks H, Bucknor A, Roussakis E, Nowell N, Kamali P, Cascales JP, Kazei D, Lin SJ, Evans CL, Science Advances 2020, 6, eabd1061. [PubMed: 33355131]

[106]. Matoori S, Veves A, Mooney DJ, Science translational medicine 2021, 13, eabe4839. [PubMed: 33731435]

[107]. Trengove NJ, Langton SR, Stacey MC, Wound Repair and Regeneration 1996, 4, 234. [PubMed: 17177819]

[108]. Li H, Guo C-Y, Xu C-L, Biosensors and Bioelectronics 2015, 63, 339. [PubMed: 25113052]

[109]. Ohayon D, Nikiforidis G, Savva A, Giugni A, Wustoni S, Palanisamy T, Chen X, Maria IP, Di Fabrizio E, Costa PMFJ, McCulloch I, Inal S, Nature Materials 2020, 19, 456. [PubMed: 31844278]

[110]. Keefe AJ, Jiang S, Nature Chemistry 2012, 4, 59.

[111]. Torrente-Rodriguez RM, Lukas H, Tu J, Min J, Yang Y, Xu C, Rossiter HB, Gao W, Matter 2020, 3, 1981. [PubMed: 33043291]

[112]. Tu J, Torrente-Rodríguez RM, Wang M, Gao W, Advanced Functional Materials 2020, 30, 1906713.

[113]. Torrente-Rodriguez RM, Tu J, Yang Y, Min J, Wang M, Song Y, Yu Y, Xu C, Ye C, IsHak WW, Gao W, Matter 2020, 2, 921. [PubMed: 32266329]

[114]. Sani ES, Wang C, Gao W, Matter 2021, 4, 2613.

[115]. Zhou J, Rossi J, Nature Reviews Drug Discovery 2017, 16, 181. [PubMed: 27807347]

[116]. Hermann T, Patel DJ, Science 2000, 287, 820. [PubMed: 10657289]

[117]. Arroyo-Currás N, Somerson J, Vieira PA, Ploense KL, Kippin TE, Plaxco KW, Proceedings of the National Academy of Sciences 2017, 114, 645.

[118]. Gao Y, Nguyen DT, Yeo T, Lim SB, Tan WX, Madden LE, Jin L, Long JYK, Aloweni FAB, Liew YJA, Tan MLL, Ang SY, Maniya SDO, Abdelwahab I, Loh KP, Chen C-H, Becker DL, Leavesley D, Ho JS, Lim CT, Science Advances 2021, 7, eabg9614. [PubMed: 34020961]

[119]. Pasche S, Angeloni S, Ischer R, Liley M, Luprano J, Voirin G, Advances in Science and Technology 2009, 57, 80.

[120]. Shastri A, McGregor LM, Liu Y, Harris V, Nan H, Mujica M, Vasquez Y, Bhattacharya A, Ma Y, Aizenberg M, Kuksenok O, Balazs AC, Aizenberg J, He X, Nature Chemistry 2015, 7, 447.

[121]. Shaw WM, Yamauchi H, Mead J, Gowers G-OF, Bell DJ, Öling D, Larsson N, Wigglesworth M, Ladds G, Ellis T, Cell 2019, 177, 782. [PubMed: 30955892]

[122]. Jaakola V-P, Griffith MT, Hanson MA, Cherezov V, Chien EYT, Lane JR, Ijzerman AP, Stevens RC, Science 2008, 322, 1211. [PubMed: 18832607]

[123]. Kwon OS, Song HS, Park TH, Jang J, Chemical Reviews 2019, 119, 36. [PubMed: 30372041]

[124]. Dörr JM, Koorengevel MC, Schäfer M, Prokofyev AV, Scheidelaar S, van der Cruijsen EAW, Dafforn TR, Baldus M, Killian JA, Proceedings of the National Academy of Sciences 2014, 111, 18607.

[125]. Ravula T, Ramadugu SK, Di Mauro G, Ramamoorthy A, Angewandte Chemie International Edition 2017, 56, 11466. [PubMed: 28714233]

[126]. Yang B, Kong J, Fang X, Talanta 2019, 204, 685. [PubMed: 31357353]

[127]. Xiong Z, Achavananthadith S, Lian S, Madden LE, Ong ZX, Chua W, Kalidasan V, Li Z, Liu Z, Singh P, Yang H, Heussler SP, Kalaiselvi SMP, Breese MBH, Yao H, Gao Y, Sanmugam K, Tee BCK, Chen P-Y, Loke W, Lim CT, Chiang GSH, Tan BY, Li H, Becker DL, Ho JS, Science Advances 2021, 7, eabj1617. [PubMed: 34797719]

[128]. Zhou J, Tun TN, Hong S.-h., Mercer-Chalmers JD, Laabei M, Young AER, Jenkins ATA, Biosensors and Bioelectronics 2011, 30, 67. [PubMed: 21945609]

[129]. Lobato IM, O'Sullivan CK, Trends Analyt Chem 2018, 98, 19.

[130]. Zhou J, Loftus AL, Mulley G, Jenkins ATA, Journal of the American Chemical Society 2010, 132, 6566. [PubMed: 20405918]

[131]. Potter M, Najer A, Klöckner A, Zhang S, Holme MN, Nele V, Che J, Massi L, Penders J, Saunders C, Doutch JJ, Edwards AM, Ces O, Stevens MM, ACS Nano 2020, 14, 17333.

[132]. Hauser AR, Nature reviews. Microbiology 2009, 7, 654. [PubMed: 19680249]

[133]. Gianino E, Miller C, Gilmore J, Bioengineering 2018, 5, 51.

[134]. Simoska O, Duay J, Stevenson KJ, ACS Sensors 2020, 5, 3547. [PubMed: 33175510]

[135]. Sheybani R, Shukla A, Biosensors and Bioelectronics 2017, 92, 425. [PubMed: 27839736]

[136]. Dao TNT, Lee EY, Koo B, Jin CE, Lee TY, Shin Y, Analytical Biochemistry 2018, 544, 87. [PubMed: 29289485]

[137]. Visuri MT, Honkonen KM, Hartiala P, Tervala TV, Halonen PJ, Junkkari H, Knuutinen N, Ylä-Herttuala S, Alitalo KK, Saarikko AM, Angiogenesis 2015, 18, 313. [PubMed: 26018927]

[138]. Emecen-Huja P, Eubank TD, Shapiro V, Yildiz V, Tatakis DN, Leblebicioglu B, J Clin Periodontol 2013, 40, 816. [PubMed: 23772674]

[139]. Bolotsky A, Butler D, Dong C, Gerace K, Glavin NR, Muratore C, Robinson JA, Ebrahimi A, ACS Nano 2019, 13, 9781. [PubMed: 31430131]

[140]. Nguyen EP, de C Carvalho Castro Silva, A. Merkoçi, Nanoscale 2020, 12, 19043. [PubMed: 32960195]

[141]. Zhang K, Jiao X, Zhou L, Wang J, Wang C, Qin Y, Wen Y, Biomaterials 2021, 276, 121040. [PubMed: 34352626]

[142]. Xu B, Li A, Wang R, Zhang J, Ding Y, Pan D, Shen Z, Advanced Functional Materials 2021, 31, 2105265.

[143]. Li H, Gu S, Zhang Q, Song E, Kuang T, Chen F, Yu X, Chang L, Nanoscale 2021, 13, 3436. [PubMed: 33538736]

[144]. Gao B, Guo M, Lyu K, Chu T, He B, Advanced Functional Materials 2021, 31, 2006839.

[145]. Zhao L, Niu L, Liang H, Tan H, Liu C, Zhu F, ACS Applied Materials & Interfaces 2017, 9, 37563. [PubMed: 28994281]

[146]. Hu C, Zhang F, Long L, Kong Q, Luo R, Wang Y, Journal of Controlled Release 2020, 324, 204. [PubMed: 32389779]

[147]. Zhu S, Nih L, Carmichael ST, Lu Y, Segura T, Advanced Materials 2015, 27, 3620. [PubMed: 25962336]

[148]. Mostafalu P, Kiaee G, Giatsidis G, Khalilpour A, Nabavinia M, Dokmeci MR, Sonkusale S, Orgill DP, Tamayol A, Khademhosseini A, Advanced Functional Materials 2017, 27, 1702399.

[149]. Mostafalu P, Tamayol A, Rahimi R, Ochoa M, Khalilpour A, Kiaee G, Yazdi IK, Bagherifard S, Dokmeci MR, Ziaie B, Sonkusale SR, Khademhosseini A, Small 2018, DOI: 10.1002/smll.201703509e1703509.

[150]. Kiaee G, Mostafalu P, Samandari M, Sonkusale S, Advanced Healthcare Materials 2018, 7, 1800396.

[151]. Xu G, Lu Y, Cheng C, Li X, Xu J, Liu Z, Liu J, Liu G, Shi Z, Chen Z, Zhang F, Jia Y, Xu D, Yuan W, Cui Z, Low SS, Liu Q, Advanced Functional Materials n/a, 2100852.

[152]. Zhao X, Liu Y, Shao C, Nie M, Huang Q, Li J, Sun L, Zhao Y, Advanced Science 2019, 6, 1901280. [PubMed: 31637165]

[153]. Li W-P, Su C-H, Wang S-J, Tsai F-J, Chang C-T, Liao M-C, Yu C-C, Vi Tran T-T, Lee C-N, Chiu W-T, Wong T-W, Yeh C-S, ACS Nano 2017, 11, 5826. [PubMed: 28521102]

[154]. Chen H, Cheng Y, Tian J, Yang P, Zhang X, Chen Y, Hu Y, Wu J, Science Advances 2020, 6, eaba4311. [PubMed: 32440554]

[155]. Pang Q, Lou D, Li S, Wang G, Qiao B, Dong S, Ma L, Gao C, Wu Z, Advanced science (Weinheim, Baden-Wurttemberg, Germany) 2020, 7, 1902673.

[156]. Wang X-F, Li M-L, Fang Q-Q, Zhao W-Y, Lou D, Hu Y-Y, Chen J, Wang X-Z, Tan W-Q, Bioactive Materials 2021, 6, 230. [PubMed: 32913931]

[157]. Ershad F, Thukral A, Yue J, Comeaux P, Lu Y, Shim H, Sim K, Kim N-I, Rao Z, Guevara R, Contreras L, Pan F, Zhang Y, Guan Y-S, Yang P, Wang X, Wang P, Wu X, Yu C, Nature Communications 2020, 11, 3823.

[158]. Long Y, Wei H, Li J, Yao G, Yu B, Ni D, Gibson ALF, Lan X, Jiang Y, Cai W, Wang X, ACS Nano 2018, 12, 12533. [PubMed: 30488695]

[159]. Yu X, Wang S, Zhang X, Qi A, Qiao X, Liu Z, Wu M, Li L, Wang ZL, Nano Energy 2018, 46, 29.

[160]. Mao C, Xiang Y, Liu X, Cui Z, Yang X, Yeung KWK, Pan H, Wang X, Chu PK, Wu S, ACS Nano 2017, 11, 9010. [PubMed: 28825807]

[161]. Du S, Zhou N, Xie G, Chen Y, Suo H, Xu J, Tao J, Zhang L, Zhu J, Nano Energy 2021, 85, 106004.

[162]. Van Gheluwe L, Chourpa I, Gaigne C, Munnier E, Polymers (Basel) 2021, 13, 1285. [PubMed: 33920816]

[163]. Liu J, Chen Z, Wang J, Li R, Li T, Chang M, Yan F, Wang Y, ACS Applied Materials & Interfaces 2018, 10, 16315. [PubMed: 29687718]

[164]. Elsherif M, Hassan MU, Yetisen AK, Butt H, ACS Nano 2018, 12, 2283. [PubMed: 29529366]

[165]. Cheng Y, Chen Q, Guo Z, Li M, Yang X, Wan G, Chen H, Zhang Q, Wang Y, ACS Nano 2020, 14, 15161. [PubMed: 33143424]

[166]. Hu X, Yu J, Qian C, Lu Y, Kahkoska AR, Xie Z, Jing X, Buse JB, Gu Z, ACS Nano 2017, 11, 613. [PubMed: 28051306]

[167]. Yao Q, Kou L, Tu Y, Zhu L, Trends in pharmacological sciences 2018, 39, 766. [PubMed: 30032745]

[168]. Chen H, Qin Z, Zhao J, He Y, Ren E, Zhu Y, Liu G, Mao C, Zheng L, Biomaterials 2019, 225, 119520. [PubMed: 31586865]

[169]. Shen B-Q, Xu K, Liu L, Raab H, Bhakta S, Kenrick M, Parsons-Reponte KL, Tien J, Yu S-F, Mai E, Li D, Tibbitts J, Baudys J, Saad OM, Scales SJ, McDonald PJ, Hass PE, Eigenbrot C, Nguyen T, Solis WA, Fuji RN, Flagella KM, Patel D, Spencer SD, Khawli LA, Ebens A,

Wong WL, Vandlen R, Kaur S, Sliwkowski MX, Scheller RH, Polakis P, Junutula JR, Nature Biotechnology 2012, 30, 184.

[170]. Xie H, Cui Z, Wang L, Xia Z, Hu Y, Xian L, Li C, Xie L, Crane J, Wan M, Zhen G, Bian Q, Yu B, Chang W, Qiu T, Pickarski M, Duong LT, Windle JJ, Luo X, Liao E, Cao X, Nature Medicine 2014, 20, 1270.

[171]. Timko BP, Dvir T, Kohane DS, Advanced materials (Deerfield Beach, Fla.) 2010, 22, 4925.

[172]. Song B, Gu Y, Pu J, Reid B, Zhao Z, Zhao M, Nature Protocols 2007, 2, 1479. [PubMed: 17545984]

[173]. Zhao M, Song B, Pu J, Wada T, Reid B, Tai G, Wang F, Guo A, Walczysko P, Gu Y, Sasaki T, Suzuki A, Forrester JV, Bourne HR, Devreotes PN, McCaig CD, Penninger JM, Nature 2006, 442, 457. [PubMed: 16871217]

[174]. Kloth LC, Adv Wound Care (New Rochelle) 2014, 3, 81. [PubMed: 24761348]

[175]. Dolmans DEJGJ, Fukumura D, Jain RK, Nature Reviews Cancer 2003, 3, 380. [PubMed: 12724736]

[176]. Li J, Liang JY, Laken SJ, Langer R, Traverso G, Trends in Chemistry 2020, 2, 319.

[177]. Gallego-Perez D, Pal D, Ghatak S, Malkoc V, Higuita-Castro N, Gnyawali S, Chang L, Liao W-C, Shi J, Sinha M, Singh K, Steen E, Sunyecz A, Stewart R, Moore J, Ziebro T, Northcutt RG, Homsy M, Bertani P, Lu W, Roy S, Khanna S, Rink C, Sundaresan VB, Otero JJ, Lee LJ, Sen CK, Nature Nanotechnology 2017, 12, 974.

[178]. Chang L, Wang Y-C, Ershad F, Yang R, Yu C, Fan Y, Trends Biotechnol 2019, 37, 1175. [PubMed: 31072609]

[179]. Song Y, Mukasa D, Zhang H, Gao W, Accounts of Materials Research 2021, 2, 184.

[180]. Chen G, Li Y, Bick M, Chen J, Chemical Reviews 2020, 120, 3668. [PubMed: 32202762]

[181]. Wang ZL, Georgia Institute of Technology, 2011.

[182]. Bhang SH, Jang WS, Han J, Yoon J-K, La W-G, Lee E, Kim YS, Shin J-Y, Lee T-J, Baik HK, Kim B-S, Advanced Functional Materials 2017, 27, 1603497.

[183]. Kai H, Suda W, Yoshida S, Nishizawa M, Biosensors and Bioelectronics 2019, 123, 108. [PubMed: 30029842]

[184]. Krishnan SR, Su C-J, Xie Z, Patel M, Madhvapathy SR, Xu Y, Freudman J, Ng B, Heo SY, Wang H, Ray TR, Leshock J, Stankiewicz I, Feng X, Huang Y, Gutruf P, Rogers JA, Small 2018, 14, 1803192.

[185]. Yu Y, Nassar J, Xu C, Min J, Yang Y, Dai A, Doshi R, Huang A, Song Y, Gehlhar R, Ames AD, Gao W, Science Robotics 2020, 5, eaaz7946. [PubMed: 32607455]

[186]. Bandodkar AJ, You J-M, Kim N-H, Gu Y, Kumar R, Mohan AMV, Kurniawan J, Imani S, Nakagawa T, Parish B, Parthasarathy M, Mercier PP, Xu S, Wang J, Energy & Environmental Science 2017, 10, 1581.

[187]. Yang X, Wang Y, Byrne R, Schneider G, Yang S, Chemical Reviews 2019, 119, 10520. [PubMed: 31294972]

[188]. Anisuzzaman D, Wang C, Rostami B, Gopalakrishnan S, Niezgoda J, Yu Z, arXiv preprint arXiv:2009.07141 2020.

[189]. Luz CF, Vollmer M, Decruyenaere J, Nijsten MW, Glasner C, Sinha B, Clinical Microbiology and Infection 2020, 26, 1291. [PubMed: 32061798]

[190]. Veredas FJ, Luque-Baena RM, Martín-Santos FJ, Morilla-Herrera JC, Morente L, Neurocomputing 2015, 164, 112.

[191]. Ward AC, Dubey P, Basnett P, Lika G, Newman G, Corrigan DK, Russell C, Kim J, Chakrabarty S, Connolly P, Roy I, Frontiers in Bioengineering and Biotechnology 2020, 8.

[192]. Goh KH, Wang L, Yeow AYK, Poh H, Li K, Yeow JJL, Tan GYH, Nature Communications 2021, 12, 711.

[193]. Tu J, Gao W, Adv Healthc Mater 2021, 10, e2100127. [PubMed: 33870653]

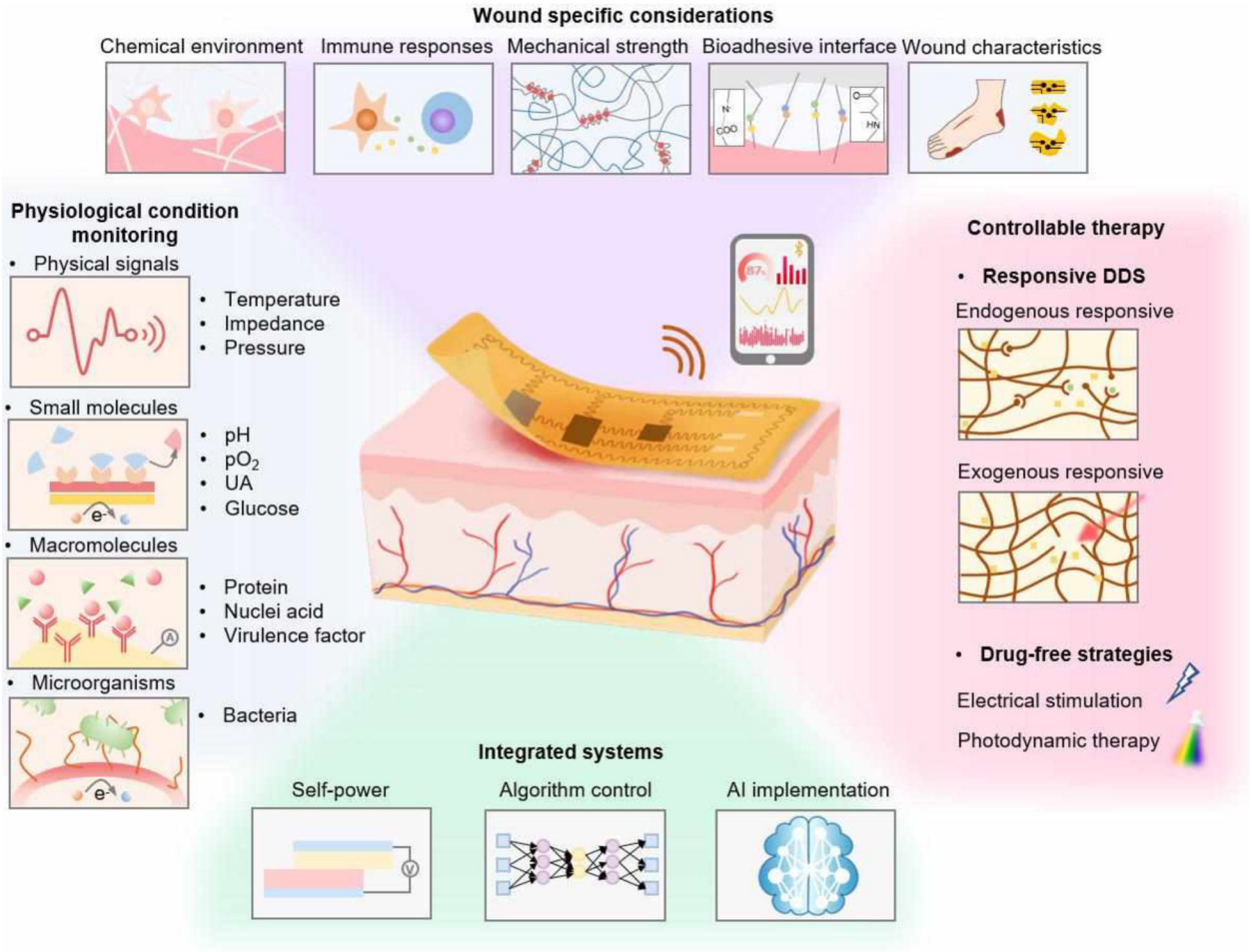

Figure 1.

Schematic illustration of wearable bioelectronics for wound biosensing and on-demand therapy administration. Wound-specific conditions should be considered to enable stable and reliable device operation. A variety of biomarkers, including physical signals, small molecules, macromolecules and microorganisms, are available in the wound milieu for wound condition assessments. Controlled by advanced algorithms, smart wearable bioelectronics could deliver therapeutic strategies such as drugs, electrical stimulation, and photodynamic therapy to the wounds responsively and timely.

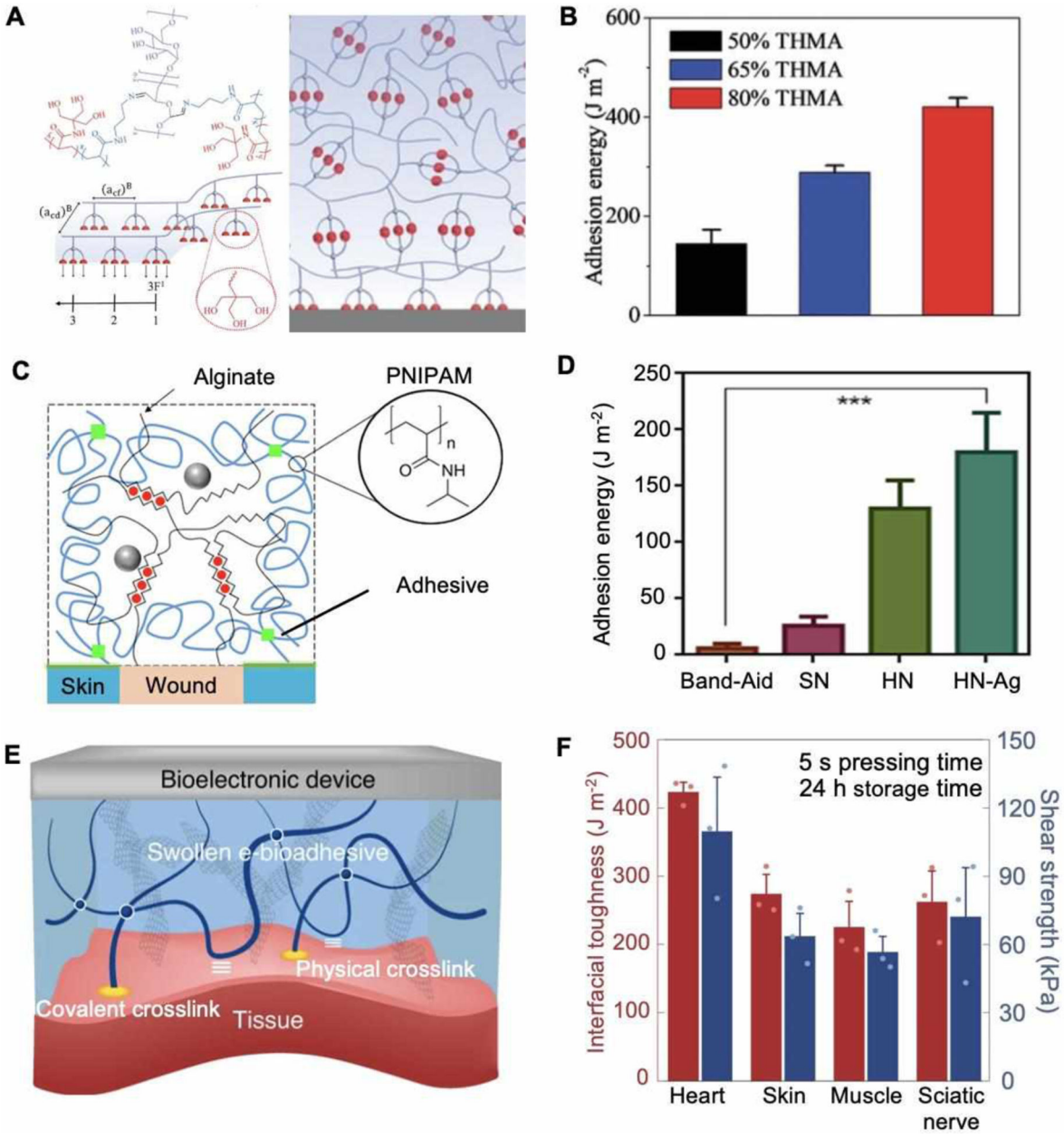

Figure 2.

Mechanical and adhesive properties for smart bandages. A. Schematic of an adhesive based on physical entanglement. B. Adhesion energy measurement of hydrogel with different formulations applied to glass slides. Reproduced with permission.[57] Copyright 2020, Wiley-VCH. C. Schematic of a covalent adhesive interface between wounds and dissipate hydrogel matrix. D. Measured adhesion energy on porcine skin. Reproduced with under the terms of the CC-BY license.[59] Copyright 2019, AAAS. E. Schematic of an e-bioadhesive interface enable interfacial fluid removement and rapid adhesion. F. Characterization of mechanical compliance and interfacial toughness on various tissues. Reproduced with permission.[61] Copyright 2020, Springer Nature.

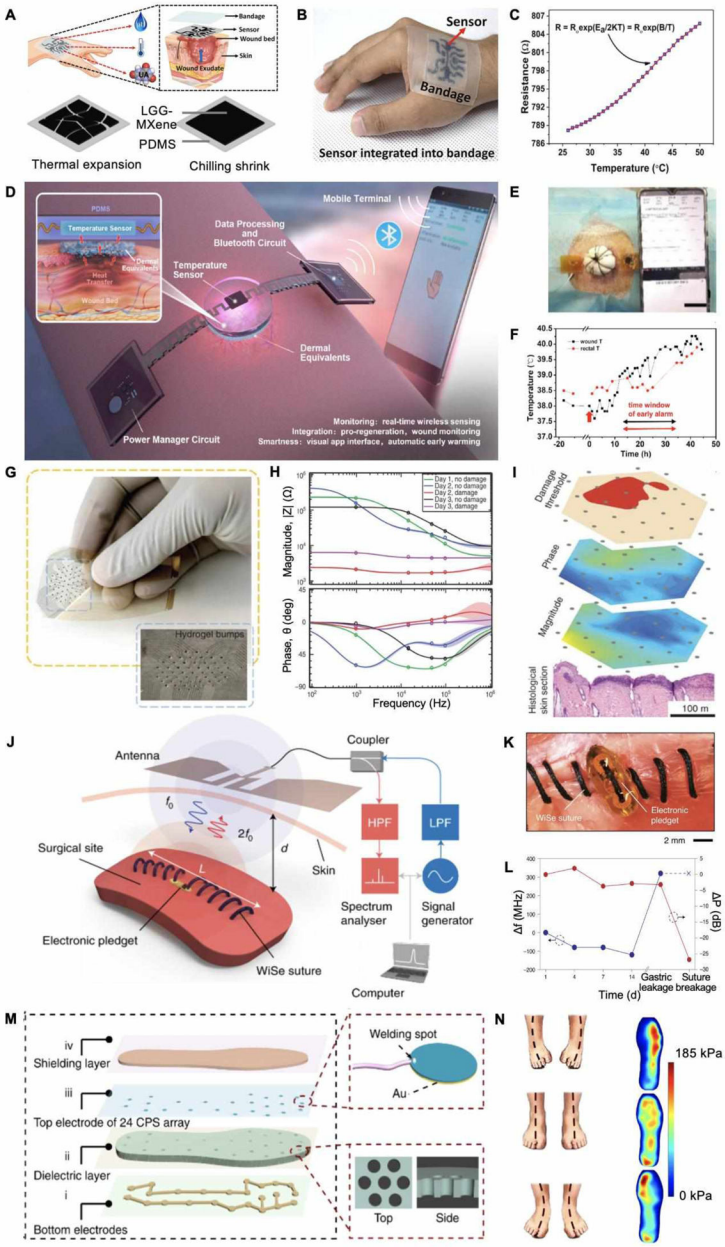

Figure 3.

Wearable physical biomarker sensing. A. Schematic of a thermosensitive material integrated wound temperature sensor. B. Photograph of applying the sensor on a human skin. C. Calibration curve of resistance as a function of temperature. Reproduced with permission.[70] Copyright 2020, Elsevier. D. A fully integrated temperature sensor and its application scenario. E. Photograph of applying the temperature sensor on a pig full-thickness wound. F. Real-time wound and rectal temperature monitoring curve of a late phase infection model. Reproduced with permission.[72] Copyright 2020, Elsevier. G. Photograph of a flexible wound impedance sensor array. H. Impedance plots of skin tissue with or without damages. I. Schematic of operating the sensor array to map skin tissue impedance. Reproduced under the terms of the CC-BY license.[73] Copyright 2015, Springer Nature.

J. Working mechanism of bioelectronic suture for wireless operation. K. Photograph of applying the suture to close muscle incision. L. Changes of signals in response to simulated gastric leakage and breakage on muscles. Reproduced with permission.[74] Copyright 2021, Springer Nature. M. Schematic and photograph of plantar pressure mapping sensor. N. Heat maps of plantar pressure with different postures. Reproduced under the terms of the CC-BY license.[75] Copyright 2020, Springer Nature.

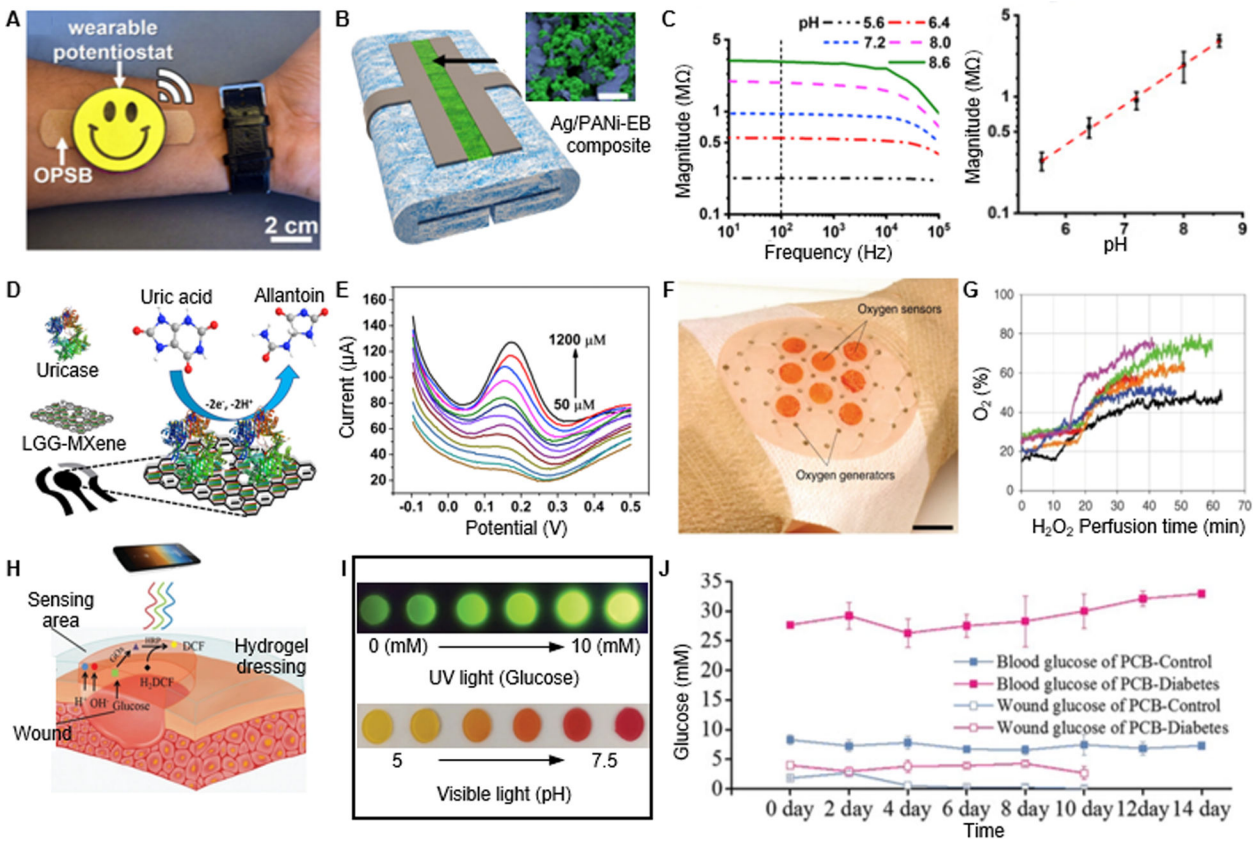

Figure 4.

Wearable small molecule sensing. A. Photograph of a wearable pH sensor with a potentiostat. B. SEM characterization of the PANI-based pH sensor. C. Calibrated impedance as a function of the pH value. Reproduced with permission.[93] Copyright 2018, Elsevier. D. Schematic of a UA sensor design. E. Uricase-based sensor response to variation of UA concentration. Reproduced with permission.[70] Copyright 2020, Elsevier. F. Photograph of a wound dressing integrated with oxygen sensors and generators. G. Oxygen measurement in response to H_2O_2 perfusion. Reproduced under the terms of the CC-BY license.[97] Copyright 2020, Springer Nature. H. Working mechanism of a colorimetric pH and glucose dual sensor. I. Images of hydrogel color changes in response to different glucose concentration or pH values. J. Measured wound glucose in comparison with blood glucose level. Reproduced with permission.[96] Copyright 2019, Wiley-VCH.

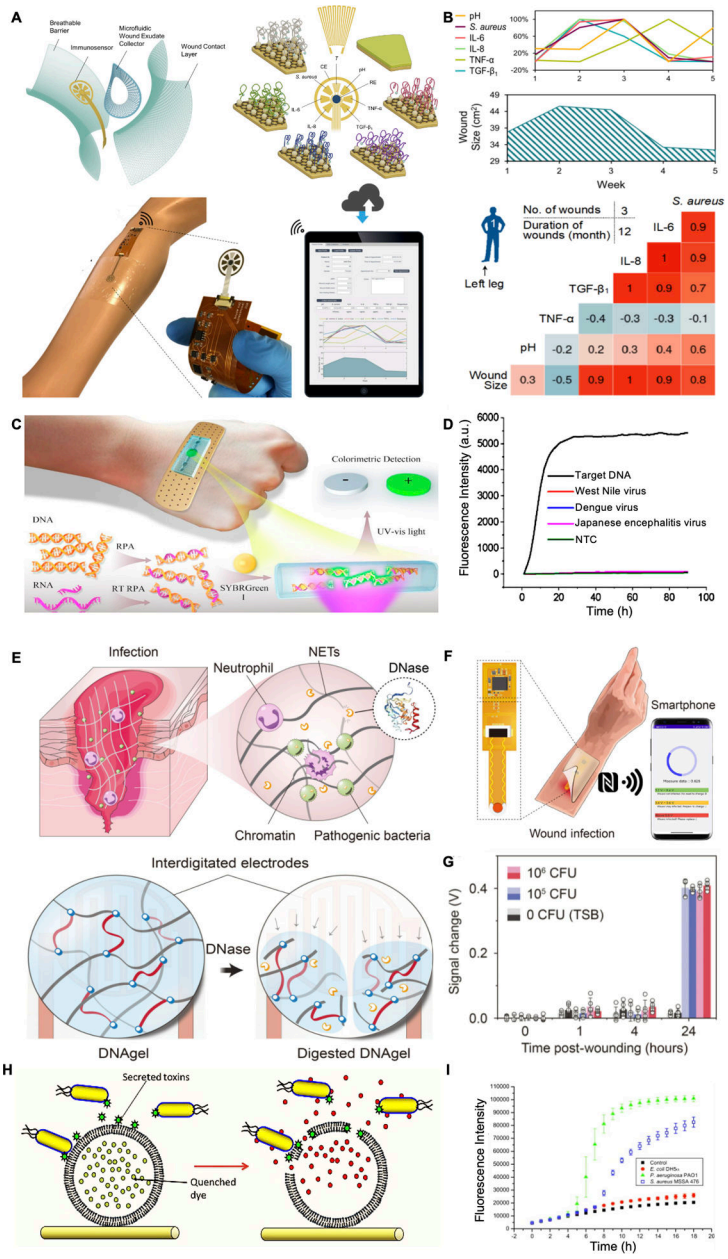

Figure 5.

Wearable macromolecule sensing. A. Schematic of an aptamer-based wound sensor integrated with wound extrude collection and wireless data transmission modules. B. Patient's fluctuations of various biomarker levels were measured and correlations among these signals were observed. Reproduced under the terms of the CC-BY license.[118] Copyright 2021, AAAS. C. Schematic of a colorimetric sensor for nucleic acid detection. D. Selective detection of target DNA against other viruses was observed. Reproduced with permission.[126] Copyright 2018, Elsevier. E. Schematic of a DNase sensing hydrogel for pathogen detection. F. Schematic of DNA gel integrated device with wireless communication module for data transfer. G. Signal changes of DNA hydrogel on control and *S. aureus* infected mice wound models. Reproduced under the terms of the CC-BY-

NC license.[127] Copyright 2021, AAAS. H. Mechanism of sensing toxins released by bacteria for wound infection detection. I. Fluorescence intensity variation of bacterial-sensitive dressing in response to the growth of different bacterial species. Reproduced with permission.[128] Copyright 2011, Elsevier.

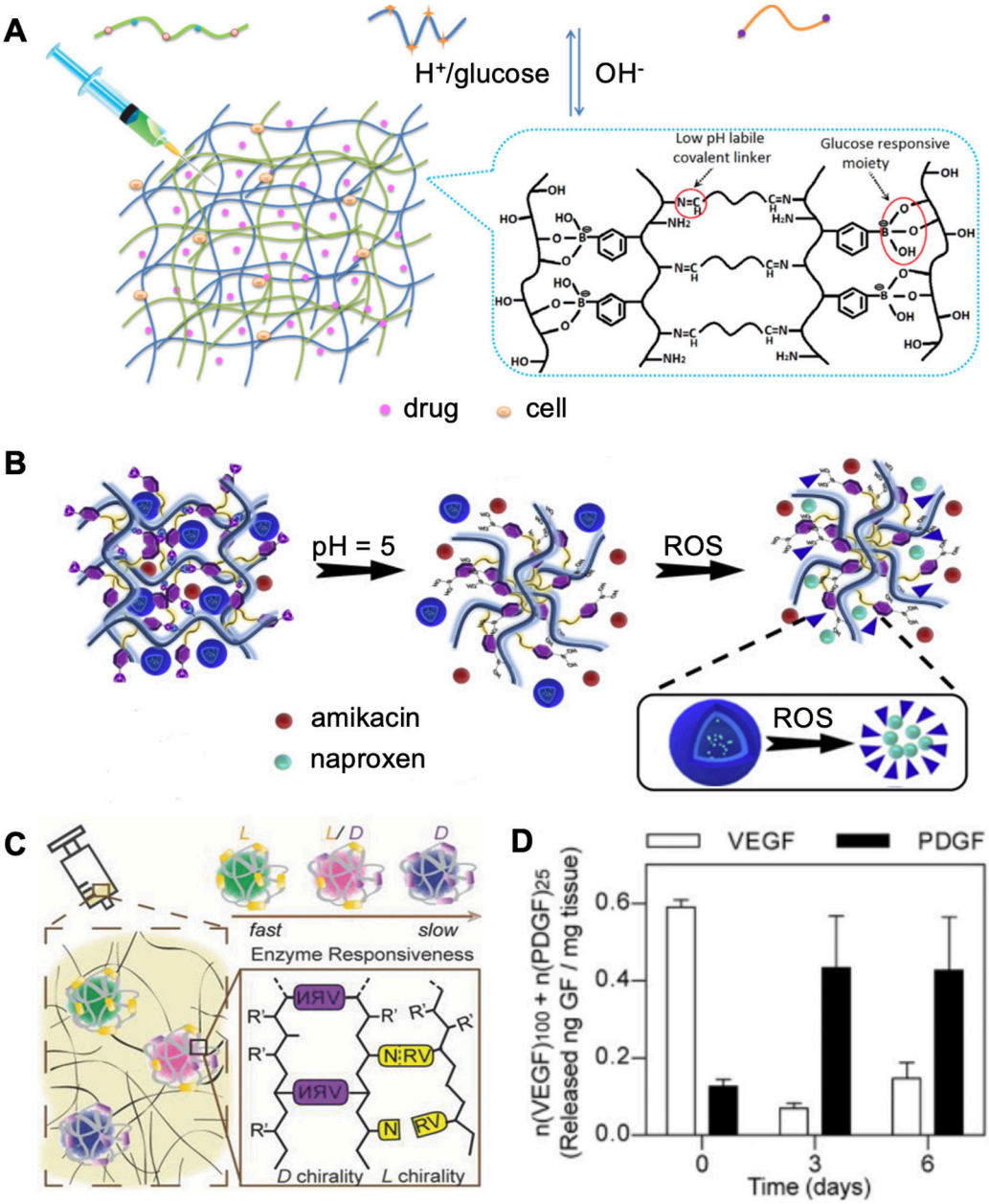

Figure 6.

Endogenously responsive drug delivery. A. Schematic of a pH and glucose dual-responsive hydrogel design for glucose and L929 fibroblast cell delivery. Reproduced with permission.[145] Copyright 2017, American Chemical Society. B. Schematic of a pH and ROS responsive hydrogel for antibiotics and anti-inflammatory drug delivery. Reproduced with permission.[146] Copyright 2020, Elsevier. C. Design of a plasmin-responsive hydrogel for growth factor sequential delivery. D. Sequential growth factor release in diabetic mouse wound models. Reproduced with permission.[147] Copyright 2015, Wiley-VCH.

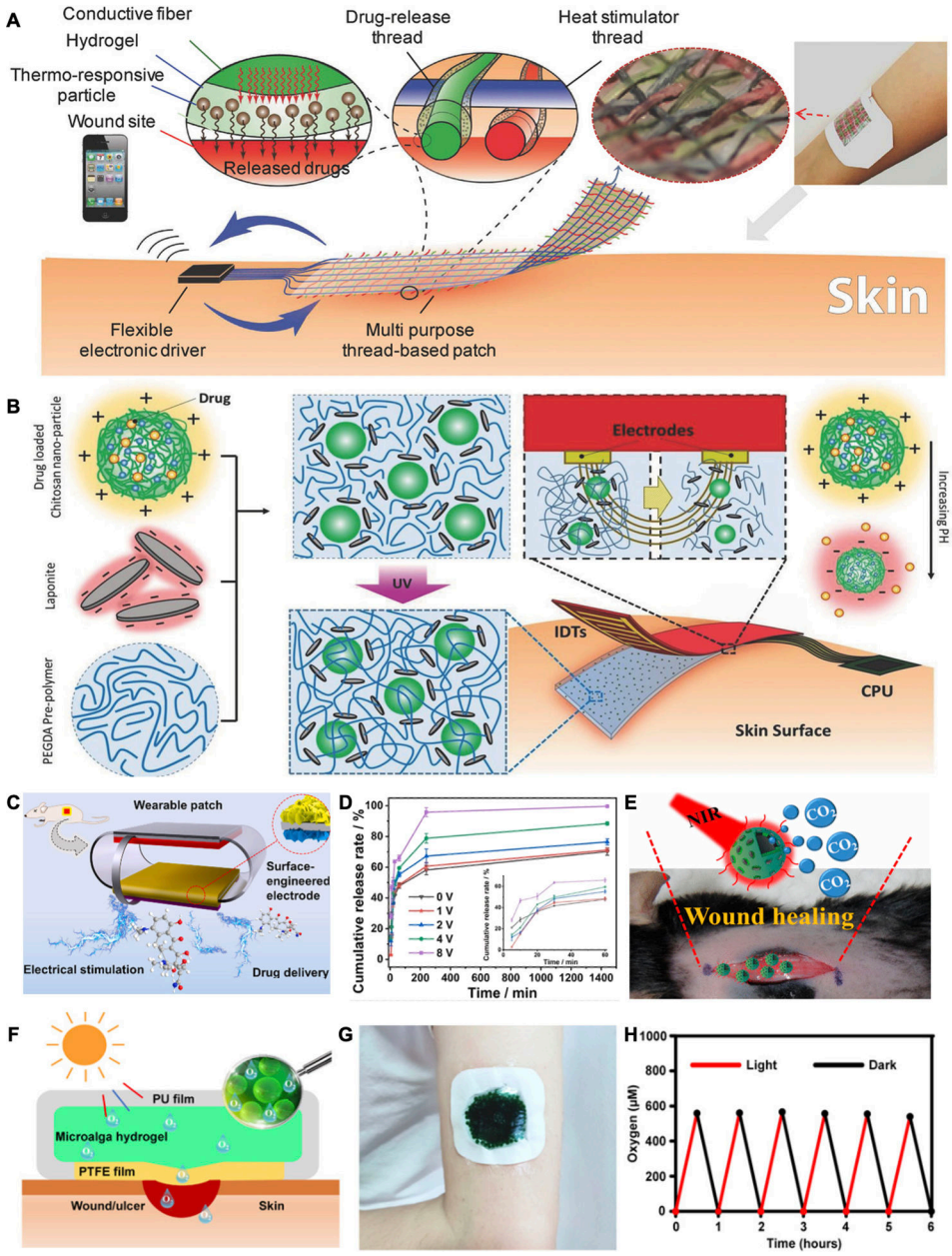

Figure 7.

Exogenously responsive drug delivery. A. Schematic of a wireless heat-responsive woven dressing for controllable drug release. Reproduced with permission.[148] Copyright 2017, Wiley-VCH. B. A electrical simulation-controlled wound patch for pH-responsive drug delivery. Reproduced with permission.[150] Copyright 2018, Wiley-VCH. C. Schematic of an electrically controlled drug release system coupling with electrical stimulation wound therapy. D. Electrical potential related drug release rates were observed. Reproduced with permission.[161] Copyright 2021, Elsevier. E. Design of NIR irradiation-mediated CO_2 delivery for wound treatment. Reproduced with permission.[153] Copyright 2017, American Chemical Society. F. Schematic of a light responsive microalga hydrogel dressing for oxygen delivery. G. Photograph of a microalga hydrogel patch adhered to a subject's arm. H.

Comparison of wound healing process by applying with alga-gel patch and other treatments for oxygen delivery on mouse. Reproduced under the terms of the CC-BY-NC license.[154] Copyright 2020, AAAS.

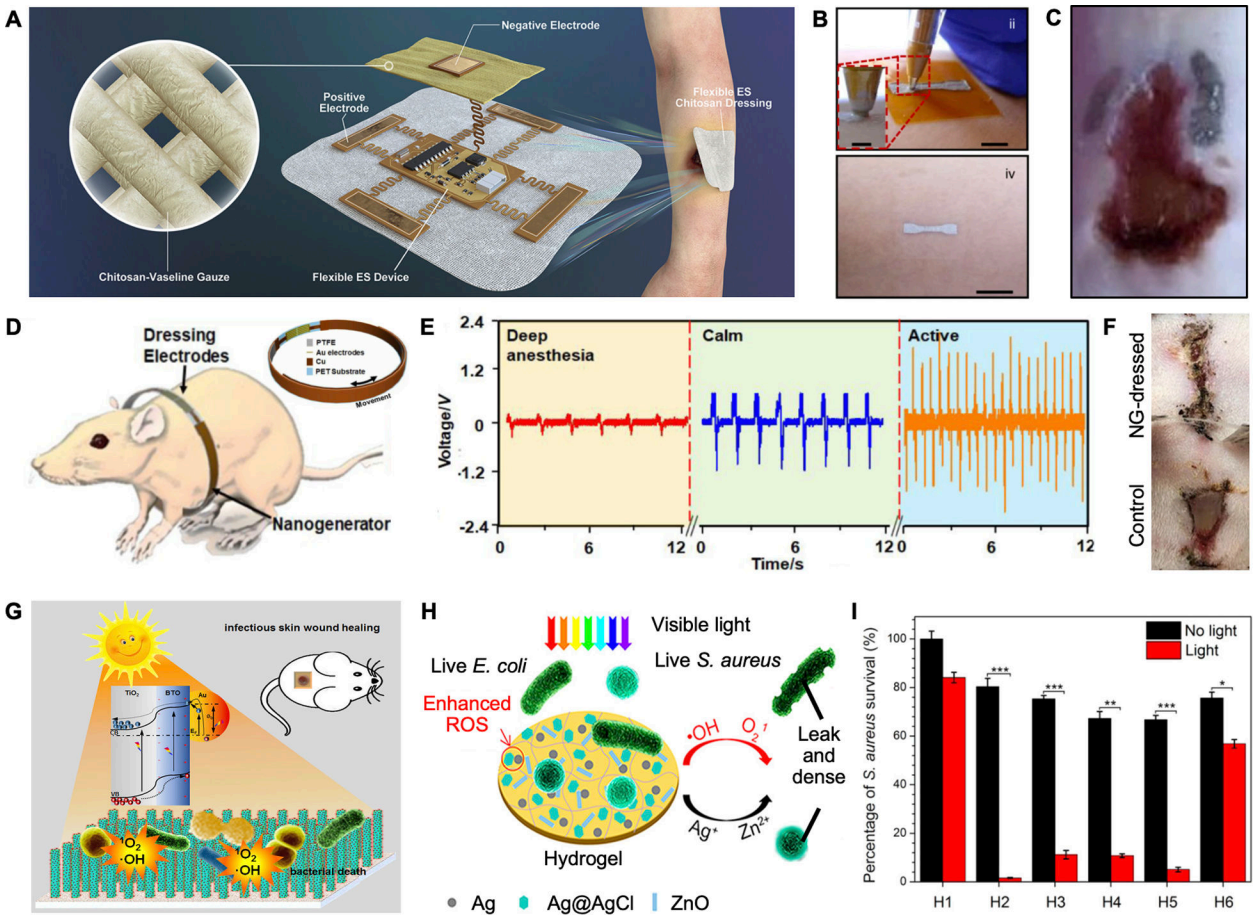

Figure 8.

Electrical stimulation and photodynamic therapy. A. Schematic and photograph of a high-voltage monophase pulsed wound dressing. Reproduced under the terms of the CC-BY license.[156] Copyright 2021, Elsevier. B. Photograph of patterning DoS electronics on a subject's skin. C. Photograph of applying low-voltage electrical stimulation on a mice wound model. Reproduced under the terms of the CC-BY license.[157] Copyright 2020, Springer Nature. D. A nanogenerator-powered bandage for electric simulation. E. Voltages generated from various rat body motions. F. Representative images of the healing process after treating with or without EF after 3 days. Reproduced with permission.[158] Copyright 2018, American Chemical Society. G. Schematic of a TiO_2-based nanoarray generating ROS to kill bacteria. Reproduced with permission.[159] Copyright 2018, Elsevier. H. Schematic of a hydrogel matrix containing ZnO and Ag for photodynamic therapy. I. Light-responsive S. aureus damage were observed with different hydrogel formulations. Reproduced with permission.[160] Copyright 2017, American Chemical Society.

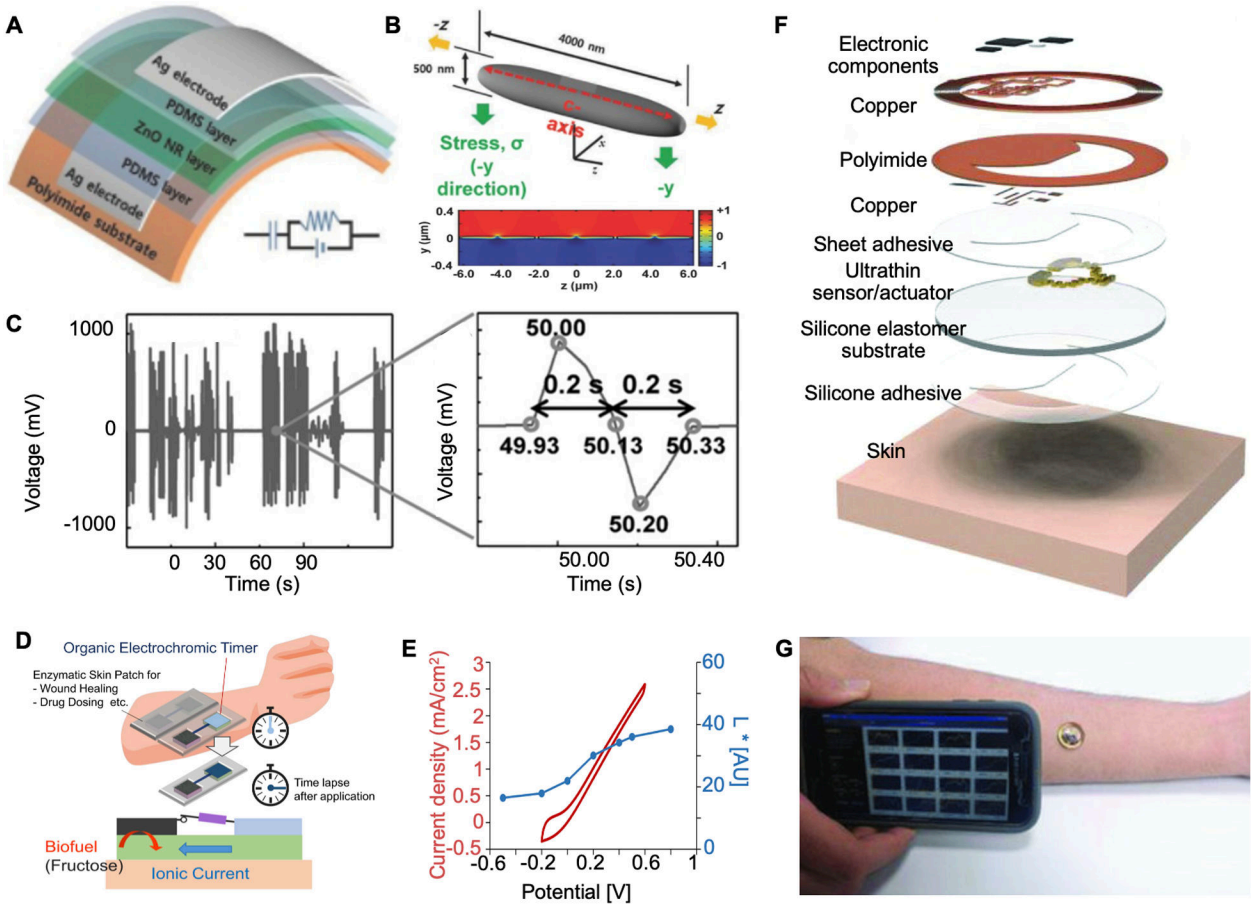

Figure 9.

Self-powered bandages. A. Photograph of the piezoelectric patch applied on wound for active wound therapy. B. Schematic illustration and calculation of the piezoelectric potential generated from the wound patch. C. Piezoelectric voltage generated by animal motions. Reproduced with permission. Reproduced with permission.[182] Copyright 2016, Wiley-VCH. D. Operation concept of a wound patch integrated with a biofuel powered electrochromic timer for drug dosing. E. Quantification of the color depth and CV current of BFC. Reproduced with permission.[183] Copyright 2019, Elsevier. F. Schematic of an NFC-based wound sensor. G. Photograph of applying the NFC sensor on a human's arm and realize wireless data transmission. Reproduced with permission. Reproduced with permission.[184] Copyright 2018, Wiley-VCH.

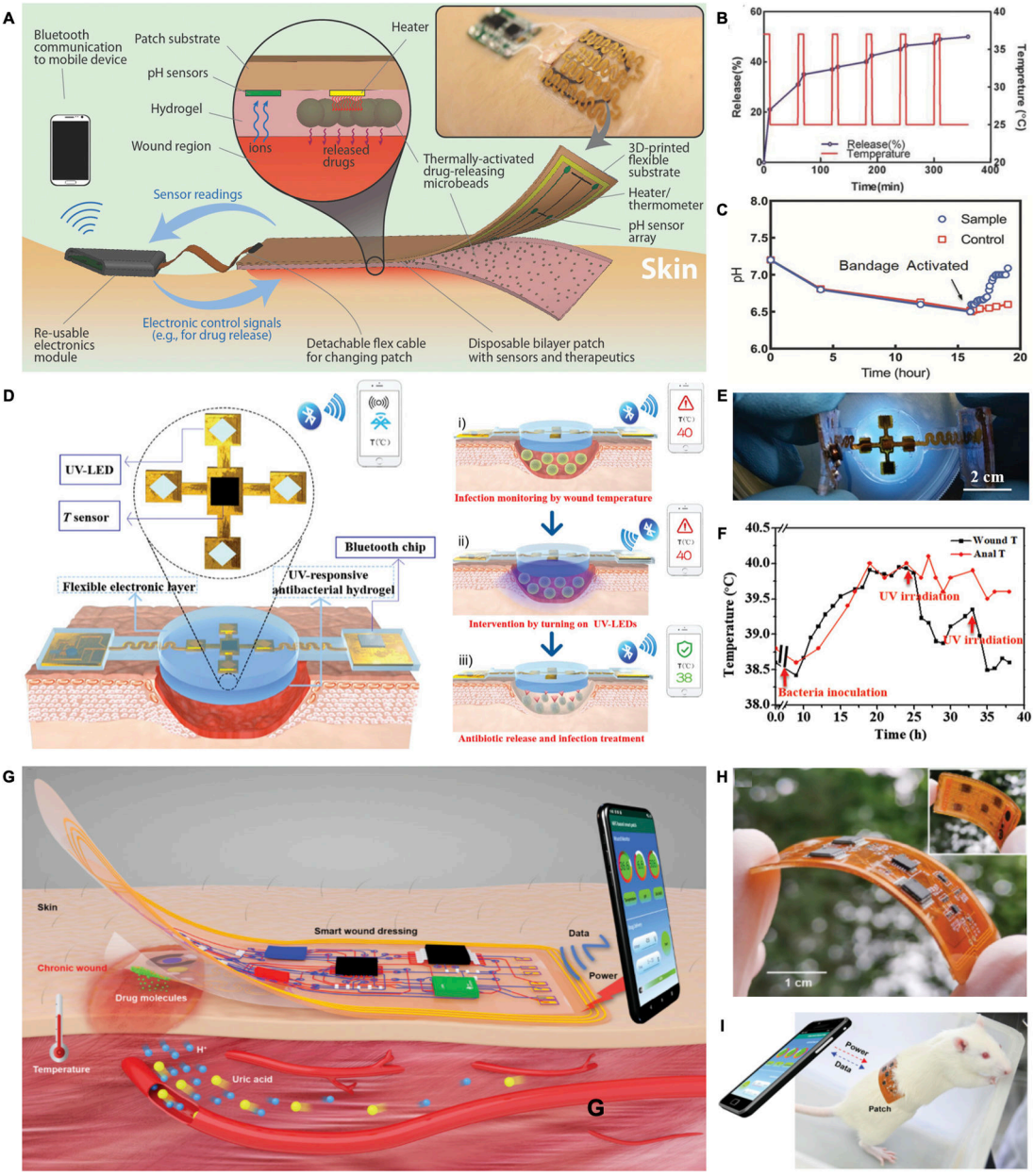

Figure 10.

Algorithm-assisted closed-loop wound management systems. A. Schematic and photograph (inset) of a closed-loop drug delivery system for infection sensing and responsive antibiotics release. Reproduced with permission.[149] Copyright 2018, Wiley-VCH. B. Schematic diagram of a smart electronic patch that controls UV-triggered drug release based on pH sensors. C. Photograph of the UV controllable closed loop wound patch. D. Real-time temperature monitoring and responsive drug release after bacterial inoculation at the wound site using anal temperature as a reference. Reproduced under the terms of the CC-BY license.[155] Copyright 2020, Wiley-VCH. E. Schematic of a wireless closed-loop wound patch that is powered by a smartphone for pH, temperature, and uric acid as well as controlled drug delivery. F. Photograph of a flexible and wireless wound patch. G. Image

of the wound patch adhered on a rat wound with an NFC-enabled data transmission. Reproduced with permission.[151] Copyright 2021, Wiley-VCH.

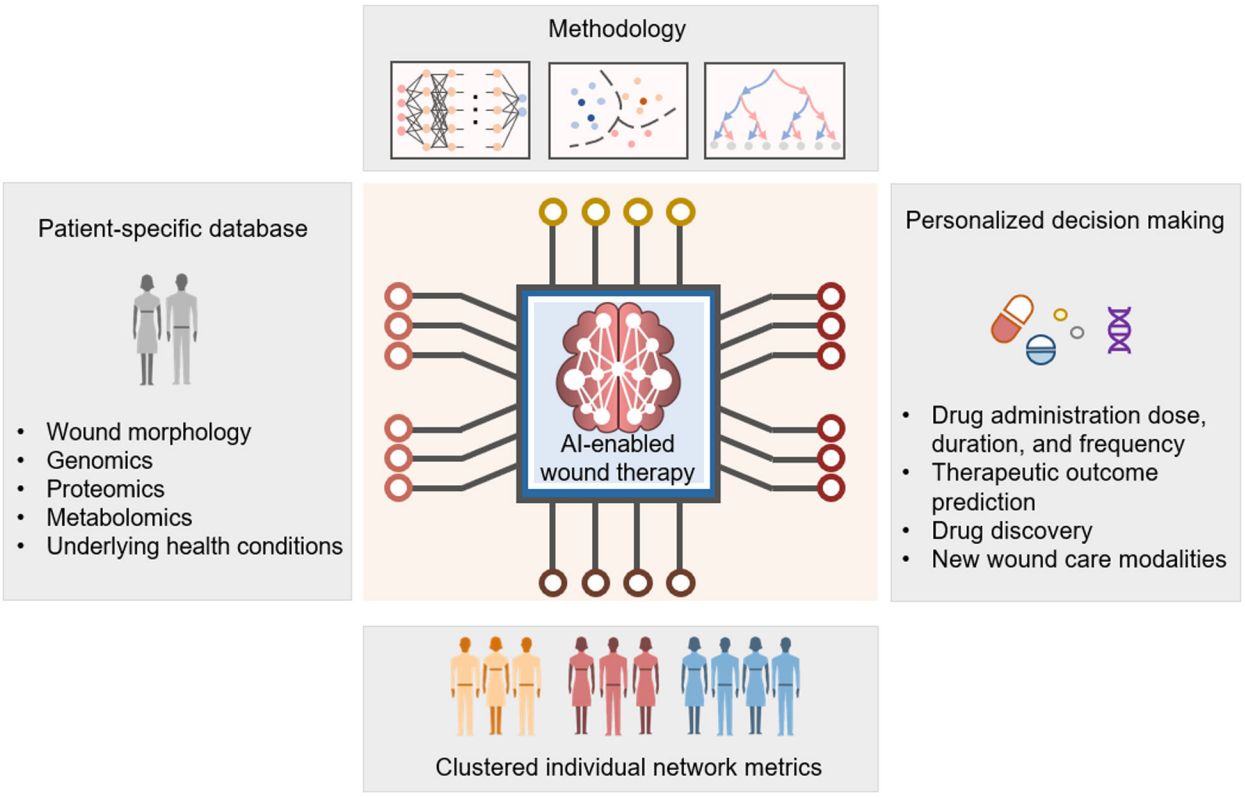

Figure 11.

Perspective of AI-implemented wearable bioelectronics for future wound management. Patient-specific database would be established and incorporate multiplexed information of patients and wound conditions. Advanced training methodologies would be involved to process diverse samples to generate clustered individual network metrics and identify patterns from previous occurrences. With AI-enabled rapid and accurate interpretations, personalized therapeutic decisions could be made to improve therapeutic efficiency and accelerate the advancement of new wound care modalities development.

Table 1.

Comparison of different treatment methods for chronic wounds.

Treatment method	Triggers	Active components	Advantages	Challenges	Ref.
Endogenously responsive DDS	Temperature	VEGF	• Convenient • Minimal patient intervention	• Loading capacity • Hard to control drug releasing timing and velocities • Limited physiological condition changes to trigger efficient drug release • Longevity challenge	[141]
	pH, glucose	Insulin and fibroblasts			[142]
	pH, ROS	Naproxen			[143]
	MMP	VEGF, PGDF			[144]
	H_2O_2	O_2			[96]
Exogenously responsive DDS	Temperature	VEGF	• Precise control of drug release	• Loading capacity • Longevity challenge • May be interfered by wound condition changes • Some stimuli can damage tissue	[145]
	Temperature	Cefazolin			[146]
	Electrical stimulation, pH	N/A			[147]
	Electrical stimulation	Cefazolin			[148]
	NIR radiation	VEGF			[149]
	NIR radiation	CO_2			[150]
	Light	O_2			[151]
	UV-light	Gentamicin			[152]
Electrical stimulation	High-voltage monophase pulsed currents	N/A	• Minimal side effects • Long-term durability • Many clinical evidence supports	• Single function	[153]
	Low-voltage electrical stimulation	N/A			[154]
	Nanogenerator -based electrical stimulation	N/A			[155]
Photodynamic therapy	Light	N/A	• Many clinical evidence supports • Avoid antibiotic resistance • Long-term durability	• Single function • Cytotoxicity of some components	[156–157]
Combined (Electrical stimulation and exogenously responsive DDS)	Nanogenerator -based electrical stimulation	Minocycline	• Combined treatment method for multiple purposes	• Interference between electrical therapy and drug release	[158]